Lesion-Induced Accumulation of Platelets Promotes Survival of Adult Neural Stem / Progenitor Cells

Ilias Kazanis[1,2+], Martina Feichtner[3,4,5+], Simona Lange[3,4], Peter Rotheneichner[4,6], Stefan Hainzl[7], Michaela Öller[4,5], Katharina Schallmoser[4,5], Eva Rohde[4,5], Herbert A. Reitsamer[4,8], Sebastien Couillard-Despres[4,6], Hans-Christian Bauer[4,9], Robin J. M. Franklin[1], Ludwig Aigner[3,4#], Francisco J. Rivera[1,3,4#*]

[1]Wellcome Trust and MRC Cambridge Stem Cell Institute & Department of Veterinary Medicine, University of Cambridge, Cambridge, United Kingdom.
[2]Department of Biology, University of Patras, Patras, Greece.
[3]Institute of Molecular Regenerative Medicine, Paracelsus Medical University Salzburg, Salzburg, Austria.
[4]Spinal Cord Injury and Tissue Regeneration Center Salzburg, Paracelsus Medical University
[5]Department of Blood Group Serology and Transfusion Medicine, Federal Hospital and Paracelsus Medical University Salzburg, Salzburg, Austria.
Salzburg, Salzburg, Austria.
[6]Institute of Experimental Neuroregeneration, Paracelsus Medical University Salzburg, Salzburg, Austria.
[7]Division of Molecular Dermatology and EB House Austria, Department of Dermatology, Paracelsus Medical University Salzburg, Salzburg, Austria.
[8]Ophthalmology/Optometry and Research Program for Experimental Ophthalmology, Paracelsus Medical University, Salzburg, Austria
[9]Institute of Tendon and Bone Regeneration, Paracelsus Medical University Salzburg, Salzburg, Austria.

[+] shared first authorship
[#] shared senior authorship

Running title: Platelets enlarge the pool of SEZ-derived NSPCs

[*] **Correspondence**
Dr. Francisco J. Rivera
Paracelsus Medical University Salzburg
Institute of Molecular Regenerative Medicine
Strubergasse 21,
Salzburg, 5020
Austria
Phone: +43 (0)662 / 44 2002 - 1281
Fax: +43 (0)662 / 44 2002 - 1223
Email: francisco.rivera@pmu.ac.at

Disclosure:

This manuscript is the peer-reviewed version of the article Ilias Kazanis, Martina Feichtner, Simona Lange, Peter Rotheneichner, Stefan Hainzl, Michaela Öller, Katharina Schallmoser, Eva Rohde, Herbert A. Reitsamer, Sebastien Couillard-Despres, Hans-Christian Bauer, Robin J. M. Franklin, Ludwig Aigner, Francisco J. Rivera (2015). Lesion-Induced Accumulation of Platelets Promotes Survival of Adult Neural Stem / Progenitor Cells. Experimental Neurology 269:75-89. doi: 10.1016/j.expneurol.2015.03.018. Epub 2015 Mar 24. The final publication is available http://www.sciencedirect.com/science/article/pii/S0014488615000862.

Abstract

The presence of neural stem/progenitor cells (NSPCs) in specific areas of the central nervous system (CNS) supports tissue maintenance as well as regeneration. The subependymal zone (SEZ), located at the lateral ventricle's wall, represents a niche for NSPCs and in response to stroke or demyelination becomes activated with progenitors migrating towards the lesion and differentiating into neurons and glia. The mechanisms that underlie this phenomenon remain largely unknown. The vascular niche and in particular blood-derived elements such as platelets, has been shown to contribute to CNS regeneration in different pathological conditions. Indeed, intracerebroventricularly administrated platelet lysate (PL) stimulates angiogenesis, neurogenesis and neuroprotection in the damaged CNS. Here, we explored the presence of platelets in the activated SEZ after a focal demyelinating lesion in the corpus callosum of mice and we studied the effects of PL on proliferating SEZ-derived NSPCs *in vitro*. We showed that the lesion-induced increase in the size of the SEZ and in the number of proliferating SEZ-resident NSPCs correlates with the accumulation of platelets specifically along the activated SEZ vasculature. Expanding on this finding, we demonstrated that exposure of NSPCs to PL *in vitro* led to increased numbers of cells by enhanced cell survival and reduced apoptosis without differences in proliferation and in the differentiation potential of NSPCs. Finally, we demonstrate that the accumulation of platelets within the SEZ is spatially correlated with reduced numbers of apoptotic cells when compared to other periventricular areas. In conclusion, our results show that platelet-derived compounds specifically promote SEZ-derived NSPC survival and suggest that platelets might contribute to the enlargement of the pool of SEZ NSPCs that are available for CNS repair in response to injury.

Key words: CNS damage; Subependymal Zone; Subventricular Zone; Vascular Niche; Platelets; Neural Stem / Progenitor Cells; Cell Survival.

Introduction

The adult CNS is generally referred to as being a tissue with restricted capacity for regeneration. However, during the last decades several studies have identified different types of CNS-resident neural stem/progenitor cells (NSPCs) that support cell turnover during homeostasis as well as regeneration (Deng et al 2010, Franklin & Ffrench-Constant 2008, Kazanis 2013). NSPCs reside in specialized microenvironments called stem cell niches that are located in the subgranular zone of the hippocampal dentate gyrus and in the subependymal zone (SEZ) of the lateral wall of the lateral ventricles (Alvarez-Buylla & Garcia-Verdugo 2002, Doetsch & Scharff 2001, Gage 2000). The main output of the rodent, but not of the adult human, SEZ is neuronal precursors that migrate along the rostral migratory stream (RMS) towards the olfactory bulb (OB), where they differentiate into functionally integrating granule and periglomerular neurons (Carleton et al 2003, Doetsch & Scharff 2001, Lois et al 1996). Apart from normal cell turnover regeneration also takes place within the adult rodent CNS; an interesting example being the re-establishment of myelin sheaths along neuronal axons in response to demyelination. In this case remyelination is driven by oligodendrocyte progenitor cells (OPCs) that are widely spread throughout the white and grey matter, and represent 5 to 8% of total glial cells (Franklin & Kotter 2008, Levine et al 2001). Furthermore, after demyelination in the corpus callosum (CC), SEZ-resident NSPCs also generate OPCs that are recruited to the lesion (Gonzalez-Perez et al 2009, Menn et al 2006, Picard-Riera et al 2002). The SEZ has also been shown to become activated in experimental models of stroke with enhancement of proliferation of NSPCs that subsequently migrate towards the lesion (Hayon et al 2012b, Kazanis et al 2013, Thored et al 2007). Although the post-injury activation of the SEZ has been described in several animal models, it is still not clear which cellular and molecular cues are involved.

Recently, platelets have been implicated in degenerative as well as regenerative processes in the CNS. Platelets are small, oval, circulating, anucleate cells that form the haemostatic plug after endothelial damage and inhibit blood leakage from vessels (Semple et al 2011). There are about one trillion platelets in the adult human circulation with a lifespan of 8 to 10 days. Bone-marrow-resident megakaryocytes daily produce approximately 100 billion of new platelets and

release them into the blood stream (Kaushansky 2006, Semple et al 2011). A plethora of bioactive molecules are stored in platelets and, under specific circumstances, are released into the extracellular space. Their function is not restricted to haemostasis, but platelets and the factors they release can exert pro-inflammatory, tissue-damaging but also tissue-regenerative activity throughout the body, including the CNS (Nurden 2011). Platelets express many surface molecules such as P2Y purinoreceptor 12, integrins αIIbβ3 and α2β1, PAR1, GPVI, glycoprotein 1b, P-selectin, EP3, $5HT_{2A}$ –receptor, thromboxane prostanoid receptor (Michelson 2010). Thus they are capable to directly interact through surface molecules with cells of the neurovascular unit (NVU) such as neurons, glial cells, endothelial cells and pericytes (Hayon et al 2013, Sotnikov et al 2013). In response to neurovascular damage they promote the infiltration of leukocytes leading to neuroinflammation, thus, contribute to the pathology (Horstman et al 2010, Langer & Chavakis 2013, Langer et al 2012, Sotnikov et al 2013, Steinman 2012). On the other hand, platelets and their derived compounds also promote neural repair, for example during corneal nerve regeneration (Li et al 2011) and after stroke (Hayon et al 2013). Based on the above and on the fact that the SEZ is characterized by a specialized vasculature, with NSPCs occupying specific positions in relation to blood vessels (Culver et al 2013, Kazanis et al 2010, Shen et al 2008, Tavazoie et al 2008) we hypothesized the existence of a direct or indirect interaction between platelets and NSPCs of the SEZ after injury.

Platelet lysate (PL) represents a cocktail of chemokines, cytokines and growth factors including among others PDGF, transforming growth factor-β (TGF-β), epidermal growth factor (EGF), basic FGF, vascular endothelial growth factor (VEGF), insulin-like growth factor (IGF)-1, and hepatocyte growth factor (HGF), as well as RNA molecules and other microparticles (Brill et al 2005, Chen et al 2012, Lohmann et al 2012, Schallmoser et al 2007, Schallmoser & Strunk 2013, Semple et al 2011, Warnke et al 2013). Thus, PL is considered to be a source of bioactive molecules that can exert a variety of physiological and pathophysiological activities. Intracerebroventricular injections of platelet lysate, for example, promote angiogenesis, neurogenesis and neuroprotection in a permanent middle cerebral artery occlusion model of stroke (Hayon et al 2013). Here, we aimed at investigating the possible involvement of platelets in the response of the SEZ to an experimental animal model of focal demyelinating lesion in the brain and to characterize *in vitro* the effects of PL on SEZ-derived NSPCs.

Materials and Methods

Animals

12-months old female C57/Bl6 mice were used for the lysolecithin-induced demyelination experiments. Their breeding and maintenance as well as the performance of all experimental procedures were done in accordance to the UK Animals (Scientific Procedures) Act 1986. 2 month-old adult female Fischer 344 rats (Charles River Deutschland GmbH, Germany) were used as donors for the NSPC cultures. All experiments were carried out in accordance with the European Communities Council Directive (86/609/EEC) and institutional guidelines. Animals had ad libidum access to food and water throughout the study.

Lysolecithin injections and tissue processing

In order to induce a focal demyelinating lesion in the corpus callosum, mice received a unilateral intracerebral injection of lysolecithin (1% in saline, 2μl injected with a Hamilton syringe at a rate of 1μl/min and then left in place for another 4min), or vehicle alone, under inhalable anaesthesia (isoflurane). The stereotaxic coordinates of the site of injection were: 0.5mm rostral and 0.8mm lateral to bregma, with lysolecithin injected at 1.5mm below the dura (within the supraventricular corpus callosum). All mice were given analgesia (Vetergesic) immediately before the injection and recovered well from the procedure. Mice were sacrificed at 4, 7 and 15 days post lesion (dpl) (n=3 mice per time-point, vehicle injected mice were sacrificed at 7dpl) by transcardial infusion of 4% paraformaldehyde (under terminal anaesthesia) and tissue was post-fixed overnight in 2% paraformaldehyde (at 4°C). Brains were subsequently immersed in 30% sucrose (in Phosphate Buffered Saline (PBS) (PAN, Germany)) for 48h (at 4°C), embedded in gelatine/ sucrose (7.5%/ 15% w/v, in PBS) and frozen at -50°C in iso-pentane (Sigma-Aldrich, UK). Sections were cut with a Leica cryostat (12*μ*m thick) and were processed for immunohistochemistry using various antibodies.

Immunohistochemistry and measurements

Fixed cryosections were washed in PBS and incubated with blocking buffer (5% Donkey Serum, 0.1% Triton x-100 from Sigma, UK, in PBS) for one hour at room temperature (RT). Sections were washed and treated with Mouse-on-Mouse immunodetection kit (Vector laboratories, BMK-2202) to avoid unspecific binding and primary antibodies were applied in blocking solution overnight 4°C. The following antibodies were used: rat anti-mouse CD41 FITC conjugated (BD Pharmingen, UK) 1:300, mouse anti-Nestin 1:100 (Abcam, UK), rabbit anti-Ki67 1:300 (Abcam, UK), rabbit anti-laminin 1:300 (Sigma, UK), rabbit anti-caspase 3 1:100 (Abcam, UK). The appropriate secondary antibodies were used, purchased from Invitrogen (Molecular probes, Alexa conjugated 488, 568 and 647 all 1:500). Nuclear counterstaining was performed with 4′, 6′-diamidino-2-phenylindole dihydrochloride hydrate 0.25 μg/μl (DAPI; Sigma, UK). Images were acquired using a Leica SP5 confocal microscope and were processed using Photoshop (Adobe CS5) and Image Processing and Analysis in Java (ImageJ) software. For the analysis of the presence of platelets periventricularly after lysolecithin-induced demyelination we used immunostaining for CD41 to label platelets and for laminin to label blood vessels. We analyzed 3 mice per time-point and at least 3 coronal sections (at the level of the lesion) per animal. The periventricular areas ipsi- and contra-lateral to the lesion were imaged by taking serial microphotographs using the 40x objective, focusing on the SEZ cytogenic niche (located along the lateral wall of the lateral ventricles) and on the non-cytogenic side (located at the medial wall)(see Figure 1A). All measurements were performed on stacks of images acquired with confocal-microscopy, in which 3 optical sections (at a 4.5 μm step) were collapsed. Measurements were performed only for vessels located in a depth of 20 μm from the ventricular wall, which is the thickness of the cytogenic niche (Kazanis et al., 2010) (Figure 1B). It has to be noted that we very rarely observed CD41+ blood vessels at higher depths from the ventricular wall. The length of each laminin+ blood vessel fragment, of each CD41+ blood vessel fragment and of the length of the ventricular wall was measured with ImageJ. Afterwards, the fraction of laminin/CD41 double-positive blood vessels per total length of blood vessels and the total length of laminin+ blood vessels per length of ventricular wall were determined. For the latter analysis the values of all areas are normalized per the value measured in the unaffected SEZ (at the unlesioned hemisphere). For total cell density, density of proliferating cells and fractions of nestin+ and caspase 3+ cells, three optical fields were imaged by con-focal microscopy with the x63 objective within the contralateral and ipsilateral SEZ and at the ipsilateral medial wall

(anatomical location of measurements is provided in Figure 10). Numbers of total Dapi+ nuclei, and of Ki67+ nuclei were counted and expressed per length of ventricular wall.

Rat NSPC cultures

Rat NSPCs were prepared as previously described (Rivera et al 2006, Sandner et al 2013). Briefly, rats were decapitated, the SEZ was dissected and collected in 4°C DPBS with 4.5 g/L glucose (Merck, Germany) (DPBS/glu). After washing the tissue, it was transferred into a petri dish and minced with a fresh sterilized razor blade. The chopped tissue was washed in DPBS/glu and resuspended in solution containing 0.01% Papain (Worthington Biochemicals, England), 0.1% Dispase II (Boehringer, Germany), 0.01% DNase I (Worthington Biochemicals, England) and 12.4 mM $MgSO^4$ in HBBS (PAN, Germany) without Mg^{2+}/Ca^{2+} (PAA, Germany). The cell suspension was digested 30 to 40 min at 37°C and every 10 min it was triturated. The cells were resuspended in Neurobasal (NB) - A medium containing B27 supplement (Gibco BRL, Germany), 2 mM L-glutamine and 100U/ml penicillin/100 µg/ml streptomycin (PAN, Germany) and washed 3 times. Finally, the cells were seeded in the same medium including 2 µg/ml heparin (Sigma, Germany), human recombinant 20 ng/ml FGF-2 (R&D Systems GmbH, Germany) and human recombinant 20 ng/ml EGF (R&D Systems GmbH, Germany). The cells were grown at 37°C in a humidified incubator with 5% CO_2. After the first 2 days in culture, and subsequently every 3^{rd} to 4^{th} day, half of the medium was changed. After 2 weeks in culture, neurospheres were passaged using Accutase (Innovative Cell Technologies Inc., distributed by PAA). Throughout this study neurosphere cultures from passage number 2 to 6 were used.

Preparation of pooled human platelet lysate (PL)

Pooled human platelet lysate (PL) was prepared as previously described (Schallmoser et al 2007, Schallmoser & Strunk 2009) using blood group O platelet concentrates of 5 days beyond expiration for clinical use. Whole blood (450 ± 45 mL) of healthy donors was collected with informed consent into a citrate phosphate dextrose containing bag system (Fresenius HemoCare Austria GmbH, Eugendorf, Austria). Each donation was screened for infections (hepatitis C virus, hepatitis B virus, human immunodeficiency virus-1 and -2, hepatitis A virus, parvovirus B19 and treponema pallidum) in accordance to the European and Austrian guidelines.

Furthermore, ABO blood groups and irregular red blood cell antibodies were tested. After a resting period of minimum 3 hours at 22°C, the whole blood sample was centrifuged (4161xg, 14 min, 22°C, Heraeus Cryofuge 6000i GMP, Thermo Fisher Scientific, Vienna, Austria) and automatically separated into plasma, red blood cells and buffy-coat layer (Compomat G4, Fresenius HemoCare, Eugendorf, Austria). After a second resting period of minimum 2 hours, 4 buffy-coat units and one plasma unit (all blood group O) were pooled and centrifuged (439xg, 8 min, 22°C, Heraeus). Platelet rich plasma was depleted from residing leucocytes by inline filtration (Pooling Set: Compostop Flex 3 F top & bottom including leucocyte filter, Fresenius) and transferred into a storage bag as platelet concentrate. Regular quality control included platelet yields, white and red blood cell contamination and pH - values. For sterility testing samples were analyzed over a period of 7 days at 36.5°C (BacT/ALERT® system, bioMérieux, Vienna, Austria). Platelet concentrates were frozen at -30°C and after at least 24h thawed at 37°C for lysis. Ten units of human platelet lysate were pooled to avoid individual donor variations. A second freeze /thaw step was performed to increase the release of active substances from platelets. Following a final centrifugation step (4000xg, 15 min, 22°C, Heraeus) and depletion of platelet fragments, PL aliquots were stored at -30°C until use.

Growth curve and cell number analysis

5 x 10^5 NSPCs were cultivated under proliferation conditions in NB-A/B27 containing L-glutamine, penicillin/streptomycin, heparin, FGF-2 and EGF (NB-A/B27 plus all) for one week (control condition). In the experimental setting PL was added in the following volume percentage: 1%, 5% and 10%. Half of the media were changed after 4 days. To evaluate the proliferation rate of the NSPCs, cell number and viability was determined by Trypan blue (Sigma Aldrich, Germany) exclusion and CASY cell counting system (Roche Applied Science, Germany). To determine the cell number by Trypan blue exclusion, 5x10^4 NSPCs were incubated in the conditions mentioned above. The cell number was quantified daily in the course of one week. Adherent NSPCs in PL conditions were rinsed and dissociated by Accutase. Neurospheres were also treated with Accutase to get a single cell suspension. Subsequently after the Accutase treatment, the NSPCs were incubated in Trypan blue for 2 min and the number of living cells was determined with a light microscope (Zeiss, Germany). To confirm these data, the cell number and viability were quantified by the CASY cell counter system as well. For CASY analysis the cell

suspension was added to CASYton solution (Roche Applied Science, Germany) in a dilution of 1:2000.

Cell Cycle Analysis

To examine the NSPC's cell cycles, Propidium Iodide FACS analysis was used. Therefore the NSPCs were cultivated in the mentioned conditions for seven days. On days 0, 4 and 7 the NSPCs were dissociated with Accutase and incubated at 37°C for 10 min. After resuspension in medium and centrifugation (4°C, 120xg, 5min) the supernatant was discarded and the cells were fixed with 1ml, -20°C cold 70% ethanol and stored at -20°C until analysis. After 3-4 days the cells were centrifuged (4°C, 120xg, 5 min), the supernatant (ethanol) was removed and the cells were resuspended in 470 µl PBS. RNase A (Promega, Germany) (4mg/ml) was added to a final concentration of 10µg/ml. After 1h of incubation at 37°C Propidium Iodide (Sigma-Aldrich, Germany) (stock 1mg/ml) was added to a final concentration of 50µg/ml. The NSPCs were vortexed and placed on ice for further analysis. Cell cycle analysis has been performed using a Gallios flow cytometer (FC 500, Beckman Coulter) and data were evaluated using Kaluza 1.2 analysis software (Beckman Coulter).

Terminal deoxynucleotidyl transferase dUTP nick end labeling (TUNEL) assay

To evaluate the apoptosis rate of NSPCs, TUNEL assay was performed. NSPCs were cultivated under the mentioned conditions for 0, 4 and 7 days. The cells were dissociated using Accutase and washed with PBS. Apoptosis was detected using In Situ Cell Death Detection Kit, TMR red (Roche) according to the manufacturer´s protocol. After washing cells were fixed with 70% ethanol at RT and permeabilized with 0.1% BSA/ 0.2% Triton X-100 in PBS for 5-10 min on ice. The samples were washed 3 times with PBS, resuspended with the TUNEL reaction solution for 1h at 37°C in the dark. Apoptotic cells were analyzed using a Gallios flow cytometer (FC500, Beckman Coulter). Kaluza 1.2 analysis software (Beckman Coulter) was used for data processing.

Marker expression profile and growth factor withdrawal

To determine the cell fate, the marker expression profile of NSPCs was analyzed. The cells were incubated in the mentioned conditions for one week. The neurospheres as well as adherent cells in PL conditions were dissociated with Accutase and seeded on 100µg/ml poly-L-ornithine (Sigma-Aldrich, Germany) and 5µg/ml laminin coated glass coverslips ($2.5x10^4$ cells/cm^2) in DMEM Knockout medium with 20% Serum Replacement supplement (SR) (Gibco Invitrogen, Germany) over night and for 7 days. As in our previous studies (Steffenhagen et al 2012, Steffenhagen et al 2011), we herein confirmed that 7 days under this condition is sufficient to achieve and analyze NSPCs differentiation, as a 10 days paradigm did not promote further development of the cells. Consistent with this, the proportion of nestin-expressing uncommitted cells dropped down from approximately 25% before the start of differentiation to 0% at 7 or 10 days after growth factor withdrawal. Similarly, the expression of progenitor markers (such as A2B5, Sox2 and DCX) was absent at 7 and 10 days of differentiation. For analysis by immunofluorescence staining the now adherent cells were fixed with 4% Paraformaldehyde (containing paraformaldehyd, 1M NaOH, ddH_2O, 1M $CaCl_2$, 1M sucrose and 0.5 M $NaPO_4$ pH7) for 20 min, washed 3 times with PBS and were stored at 4°C until further use. The cell fate was also analyzed on mRNA level. Therefore NSPCs were seeded in 100µg/ml poly-L-ornithine and 5µg/ml laminin coated petri dishes in a density of 1 x 10^6 cells in DMEM Knockout containing 20% Serum Replacement supplement (SR) (Gibco Invitrogen, Germany) over night. mRNA isolation was performed using RNeasy Plus Mini Kit (Qiagen, Germany) according to the manufacturer´s protocol.

Immunocytochemistry

The on coverslips fixed NSPCs were blocked for 2h at RT with fish skin gelatin buffer (FSGB) containing TBS (0.15 M NaCl, 0.1 M Tris-HCl, pH 7.5), 0.1% Triton-X100 (only for intracellular antigens), 1% bovine serum albumin (BSA) and 0.2% Teleostean gelatin (Sigma, Germany). Primary antibodies were applied in blocking solution overnight 4°C. Cells were incubated with fluorochrome-conjugated species-specific secondary antibodies for 2h at RT, washed twice with PBS and once with ddH_2O. To analyze the marker expression profile and the response to growth factor withdrawal the following antibodies were used. Primary antibodies: rabbit anti-glial

fibrillary acidic protein (GFAP) 1:1000 (Dako, Denmark); mouse anti-rat Nestin 1:500 (BD Pharmingen, Germany); goat anti-Sox2 1:1000 (Santa Cruz, Germany); rabbit anti-Olig2 1:300 (Millipore, USA); IgM mouse anti-A2B5 1:100 (Chemicon, UK); rabbit anti-doublecortin (DCX) 1:500 (Cell Signaling, USA); rabbit anti-Beta3 Tubulin 1:500 (Abcam, UK); mouse anti-2`, 3`-cyclic-nucleotide-3`-phosphodieesterase (CNPase) 1:200 (Millipore, USA); rabbit anti-NG2 1:200 (Millipore, USA); rabbit anti-Galactocerebroside (GalC) 1:200 (Millipore, USA); mouse anti-Myelin Basic Protein (MBP) 1:750 (Smi-94, Covance, USA); mouse anti-Map2a+2b 1:250 (Sigma Aldrich, Germany). Secondary antibodies: donkey anti-rabbit conjugated with Alexa 568 1:500 (Invitrogen, Germany); donkey anti-goat conjugated with Alexa 488 1:500 (Invitrogen, Germany); donkey anti-mouse conjugated with Alexa 488 1:500 (Invitrogen, Germany); donkey anti-IgM mouse conjugated with FITC 1:500 (Jackson ImmunoResearch, UK); donkey anti-rat conjugated with rhodamin red 1:500 (Jackson ImmunoResearch, UK). For the detergent-sensitive antigens (i.e. A2B5, GalC and NG2) Triton X-100 was omitted from FSGB. Nuclear counterstaining was performed with 4´, 6´-diamidino-2-phenylindole dihydrochloride hydrate 0.25 µg/µl (DAPI; Sigma, Germany). Specimens were mounted on microscope slides using Prolong Antifade kit (Molecular Probes, USA). Epifluorescence observation and photo documentation were realized using an Olympus IX81 (Olympus, Germany) equipped with Hamamatsu digital camera and Volocity software (Perkin Elmer, Germany). For each culture condition, 5 to 10 randomly selected observation fields, containing 300-500 cells, were photographed for cell fate analysis. The marker expression profile was determined for each condition in 3 independent experiments.

Quantitative real time polymerase chain reaction (qRT PCR)

To isolate mRNA the Quiagen RNeasy Mini Kit was used following user protocol. 1µg mRNA was retro-transcribed to cDNA using the Promega Reverse Transcription System (Promega, Germany) with random primers. To evaluate the NSPC's cell fate on mRNA level, quantitative real time polymerase chain reaction (qRT PCR) was performed. 10ng cDNA was used for PCR. The expression of DCX, Olig2 and Id2 (Applied Biosystems, USA) genes was analyzed using a GoTaq probe q PCR master mix (Promega, Germany). YWHAZ (assay ID: Rn.PT.56a.8368619, Integrated DNA Technologies, USA), Eef2 (assay ID: Rn.PT.56a.36171938.gs, Integrated DNA

Technologies, USA) and TBP (assay ID: Rn.PT.39a.22214837, Integrated DNA Technologies, USA) served as housekeeping genes. The following temperature profile was used: activation of GoTaq polymerase 50°C, 2min and 95°C 10 min; 40 cycles of denaturing 95°C, 15 s, and annealing/extension 60°C, 60 s. Data were obtained using a CFX96 Touch Real-Time PCR Detection System (Biorad, USA) and analyzed by qBase Plus (Biogazelle, Belgium). The expression of all genes of the control conditions was used as calibrators. Data was analyzed by accurate normalization using a geometric averaging of multiple internal control genes (Vandesompele et al 2002).

Statistical Analysis

Data are presented as mean values +/- SD and statistical analysis was performed with PRISM5 (GraphPad, San Diego, CA, USA). P values of < 0.05 were considered to be significant acquired by parametric one-way ANOVA-Tukey post hoc. For statistical analysis with time courses experiments two-way ANOVA-Bonferroni post hoc was used. For the statistical analysis of immunostainings on tissue sections, we performed two-way ANOVA with time and area used as independent parameters and matching values measured from the same animal. For the comparisons of CD41+ fractions of blood vessels the two-way ANOVA was followed by the Dunnett's 's post-hoc test and for the comparisons of overall laminin-expressing blood vessels the two-way ANOVA was followed by the Sidak's post-hoc test. All experiments were performed, at least, as 3 independent biological replicates.

Results

Demyelinating lesions in the supraventricular corpus callosum increase the amount of Laminin-expressing vessels, and induce a cytogenic response and an accumulation of platelets in the SEZ niche

We induced a focal demyelinating lesion in the SEZ-adjacent supraventricular corpus callosum (CC) (Nait-Oumesmar et al 1999) by injecting lysolecithin, a toxin that provokes a well-

characterized demyelinating injury (Woodruff & Franklin 1999). Subsequently we assessed the response of the periventricular area and evaluated the expression of laminin as a marker for blood vessels around the lateral ventricles (LV) (Kazanis 2013) (Figure 1A,B). The contralateral side was used as healthy internal control and vehicle-injected mice were used to control for the effects of the mechanical injury caused by the needle insertion (Figure 2). We quantified the density of laminin+ blood vessels detected at the cytogenic (lateral) and the non-cytogenic (medial) ventricular walls contralateral and ipsilateral to the lesion in order to assess the effects of the lesion to the vasculature (Figure 1). Four days post-lesion (dpl) there was no significant response of the periventricular vasculature to the lesion as judged by the similar density of laminin-expressing blood vessels in the hemispheres ipsilateral and contralateral to the lesion (Figure 1C). However, at 7 and 15 dpl we detected a significant response of the vasculature at both sides of the ipsilateral LV manifested as increased density of laminin-expressing vessels when compared to the respective contralateral areas and to 4dpl (Figure 1C). No such response was observed after vehicle injection in the CC (Figure 2). In order to assess the cell-generating response, we quantified the number of total cells and of proliferating cells in the SEZ of the lateral ventricle wall. We observed a significant increase in the size of the SEZ specifically at the affected hemisphere, as revealed by an increase in the density of total cells, both at 4 dpl (when the vasculature is not activated) and at 7 dpl (Figure 1D - F). Similarly, proliferation was significantly increased in the ipsilateral SEZ as measured by counting numbers of Ki67+ cells (Figure 1D, E and G). No increase in the density of total and proliferating cells within the ipsilateral SEZ were detected 7 days after vehicle injection (Figure 2D). Therefore, the lysolecithin-induced lesion within the CC activated the vasculature in both LV sides and induced a cytogenic response specifically in the SEZ niche.

Platelets are involved in regeneration of various tissues and organs; therefore, we sought to investigate their possible involvement in the response of SEZ-resident NSPCs after the focal demyelination in the CC. Initially we assessed if platelets could be detected in the periventricular tissue by performing immunostainings for CD41. At 4 dpl platelets were found to accumulate at the area of the lesion, both within blood vessels and, the majority, in the extravascular space of the brain parenchyma (Figure 3B and Figure 4A). When looking at higher magnification within the area of lesion, CD41 immunopositive particles with a size compatible to platelets could be found in the lumen of vessels, attached on vessel walls and migrating out of the vasculature

(Figure 4). No CD41 immunoreactivity was detected in the contralateral, unaffected, CC (Figure 2C). Notably, significant accumulation of platelets was also observed within the SEZ (Figures 2A, 3B-C, 4A) with a massive (approximately 15 to 20 times) increase in their presence when compared to the contralateral and ipsilateral-medial LV walls (Figure 3C), but also when compared to the ipsilateral medial wall of the LV in which the vasculature showed similar levels of stress-related laminin expression (Figure 1C). Unlike in the CC, platelets in the niche only formed clusters that were in close association with laminin+ vascular cells (Figure 4). Furthermore, CD41+ clusters of platelets were observed near Ki67+ nestin+ cells (i.e. in proximity to SEZ-resident proliferating NSPCs) (Figure 3D). This pattern of distribution of CD41+ platelets remained similar at all time-points investigated (4, 7 and 15 dpl, Figure 3C). Importantly, we found no sign of accumulation of platelets within the SEZ of vehicle-injected mice at 7dpl (Figure 2) indicating that a simple mechanical disruption of the CC tissue without further degenerative phenomena does not induce activation of the SEZ and accumulation of platelets within this region. Therefore, the lysolecithin-induced lesion within the CC specifically provoked platelets aggregation at the SEZ vasculature in the close proximity to proliferating NSPCs.

Platelet Lysate induces morphological changes in NSPCs and increases their cell number in vitro

Upon vascular damage, platelets release a plethora of bioactive molecules that modulate tissue repair (Semple et al 2011). Here, we aimed to investigate whether the lesion-induced accumulation of platelets might be involved in the post-lesion cytogenic activation of the SEZ. Therefore, we studied the effect of a Platelet Lysate (PL) that represents a *bona fide* source for platelet-derived molecules, on NSPCs *in vitro*. We cultured rat-derived SEZ NSPCs (grown as 3D cell aggregates called neurospheres) with 1%, 5% and 10% of PL and analyzed the effects on their morphology and on their rate of expansion in comparison to cells grown in medium without PL. With increasing dose of PL and exposure time, neurospheres attached more to the plastic surface of the culture dish changing their cell morphology (Figure 5A-L).

Next we analyzed the expansion rate over a time period of 7 days by using automated cell (CASY) as well as manual (Trypan blue exclusion) counting. PL treated cultures expanded

significantly more compared to untreated cultures (Figure 5M, N). Interestingly, the strongest effect on cell expansion was achieved with the 1% PL condition, followed by 5% PL, while 10% PL had no effect on the cell expansion rate (Figure 5M, N). In summary, PL promotes cell adhesion and cell expansion on NSPCs. While cell adhesion was most strongly promoted by the high dose of PL (10%), cell expansion was highest in the low dose of PL (1%). Thus, the two effects appear to be independent and might use different factors present in the PL.

PL does not affect the lineage commitment neither the differentiation potential of NSPC

Morphological changes in NSPCs are often associated with changes in their lineage commitment and/or to differentiation. In order to gain a comprehensive picture on the effects of platelet-derived factors on NSPCs in vitro, we analyzed their lineage commitment both in proliferating and in differentiating conditions. First, we analyzed the marker expression profile of NSPCs grown under control proliferation conditions or in the presence of 1%, 5%, 10% PL for 7 days. Under proliferative conditions rat-derived NSPCs mainly express glial progenitor markers while a small subpopulation displays neuronal progenitor features (Steffenhagen et al 2011). PL, regardless of the dosage used, did alter neither the percentage of A2B5-, NG2- and Olig2-expressing glial progenitor subpopulations (Figure 6A-L, Q, R and S) nor the DCX-expressing neuronal subpopulation (Figure 6M-P and T). As expected, proliferating NSPCs rarely expressed mature glial and neuronal markers (GFAP, GalC and Beta3-Tubulin, respectively) and PL did not influence this expression pattern (data not shown). To confirm at the mRNA level and to evaluate potential effects of PL in fate determination we analyzed the mRNA expression of the glial fate determinants Id2 (for astrocytes) and Olig2 (for oligodendrocytes) as well as of the neuroblast marker DCX by RT-PCR. PL did not induce any changes in the expression levels of any of these genes (Figure 6U-W).

In a previous study we have shown that although rat-derived NSPCs are tripotent being able to give rise to neurons, astrocytes and oligodendrocytes, they are partially committed to the oligodendroglial lineage (Steffenhagen et al 2011). Upon growth factor withdrawal, almost 80% of NSPCs give rise to mature oligodendrocytes, when placed in serum-free medium (Steffenhagen et al 2011). Here, we analyzed whether PL affects the oligodendrogenic intrinsic fate of the cells either shifting towards astrocytes / neurons or influencing their oligodendrogenic

efficiency. NSPCs were incubated in proliferation medium in the presence or absence of different PL concentrations for 7 days. After this period, cells were plated in medium supplemented with serum replacement (SR) in the absence of EGF and FGF for one week (as in (Steffenhagen et al 2012, Steffenhagen et al 2011)) and analyzed for the expression of cell type and lineage specific markers. In neither concentration, PL did influence the percentage of CNPase-, GalC- and MBP-expressing mature oligodendrocytes (Figure 7A-F) or GFAP-positive astrocytes (Figure 7G, H). Similarly, PL did not affect the percentage of DCX-expressing immature neurons that remain lower than 2%. In addition, there was no difference in the proportion of Beta3-Tubulin and MAP2a+2b-expressing neurons regardless of the condition (Figure 7 I-L). Finally, as expected, after growth factor withdrawal the proportion of NSPCs that express uncommitted or progenitor markers was negligent in all tested conditions (data not shown). Thus, PL did not have any effect on NSPCs' intrinsic fate and differentiation.

PL increases the numbers of NSPCs by specifically enhancing cell survival but without affecting proliferation and cell cycle length

The PL-induced elevated expansion rate of NSPCs might derive from enhanced proliferation or from a better survival of NSPCs in culture. To distinguish between these two possibilities we investigated the cell cycle of NSPCs grown with or without PL and quantified the percentage of NSPCs being in G0/G1 and in the G2/S/M phases of the cell cycle. Cells were grown in proliferation medium with or without 1%, 5% and 10% of PL and the cell cycle phases were examined using propidium iodide flow cytometry at day 0, 4 and 7. PL treated cultures were not different from untreated cultures in their cell cycle pattern in none of the time points investigated (Figure 8A, B). These data suggest that the PL mediated effect on NSPC expansion is not due to an enhanced proliferation rate.

Next, we investigated whether PL promotes NSPCs' survival and has a protective effect in neurosphere cultures. Therefore, cells were grown in the absence or presence of PL (1%, 5%, 10%) for 7 days and viability was evaluated by CASY cell analysis and Trypan blue exclusion. In all three concentrations tested PL significantly increased cell viability (Figure 9A, B). Next, cells were grown in the absence or presence of PL for 4 days and the percentage of apoptotic cells was determined by propidium iodide flow cytometry analysis. Results revealed a significant decrease

in the percentage of apoptotic cells after exposure to 1% and 5% PL (Figure 9C). Finally, we aimed to validate these results by an independent method, and analyzed the effects of PL on cell death using a TUNEL assay. PL reduced cell death in all three concentrations tested (Figure 9D). Again, the strongest anti-apoptotic effect was found in the 1% PL conditions, followed by 5% PL, and then 10% PL. In summary, the results clearly indicate an anti-apoptotic and protective effect of PL in NSPC cultures.

The lesion-induced accumulation of platelets in the SEZ coincides with lower numbers of apoptotic cells

Encouraged by the *in vitro* findings showing an effect of platelet-derived factors on the survival of NSPCs, we revisited the post-lesion mouse tissue in order to perform double immunostainings for activated caspase 3, a well-established marker of apoptotic cells and nestin to mark stem/ progenitor cells in the SEZ. At 4 dpl (n=4) approximately 40% of cells within the contralateral unaffected niche were nestin+ (Figure 10F) and of them almost a quarter was co-expressing caspase 3 (Figure 10H). Notably, in the SEZ ipsilateral to demyelination, although the pool of nestin+ cells was significantly expanded (58.24%±2.64% of all cells vs 37.95%±2.84% of all cells in the contralateral side), their fraction co-expressing caspase 3+ was significantly lower (14.65%±2.76% within the ipsilateral SEZ niche vs 24.93%±2.26% in the contralateral) (Figure 10F, H). In contrast, at the medial LV walls (non cytogenic areas) the number of apoptotic cells (these were not NSPCs) was significantly increased in the ipsilateral hemisphere (data not shown). Therefore, the specific accumulation of platelets in the affected SEZ was accompanied by a specific decrease in the overall occurrence of apoptotic cells (Figure 10G) including a strong decrease in apoptotic progenitors (Figure 10H).

Discussion

In the present study we investigated the influence of platelets on SEZ-NSPCs, which represent an endogenous source of cells for tissue maintenance and repair in the CNS. We showed that a focal

demyelinating lesion in the mouse CC activated the SEZ niche resulting in a significant increase in its cell density even at early post-lesion stages (at 4dpl). Also, we observed an accumulation of vessel-associated platelets within the NSPC-rich SEZ niche after the lesion. Notably, this platelets aggregation had two key characteristics: first, it occurred specifically at the cytogenic side of the lateral ventricle (in the SEZ) (Figure 3C) even though the effects of the lesion on the vasculature -as judged by the increased expression of laminin on blood vessels- was present all around the LV (Figure 1C). Second, the platelet aggregation occurred early (at 4 dpl) and, thus, correlated more with the activation of the SEZ rather than with the late appearance of the general vascular response (upregulation of laminin expression). This spatiotemporal correlation of platelet accumulation with the SEZ-resident NSPCs responses indicated the existence of an interaction between the two cell populations. This hypothesis was evaluated more in detail with our *in vitro* findings, which revealed that exposure of NSPCs to PL increased their cell number by boosting cell survival and decreasing apoptosis, without affecting cell proliferation. Indeed, the cytogenic capacity of the SEZ is determined by the balance between cell proliferation and cell death (Morshead & van der Kooy 1992) and previous experimental work has identified molecules that exert pro-survival effects on adult NSPCs without affecting proliferation (Gago et al 2003, Hunt et al 2010). In our model, the pro-survival effect of PL on NSPCs that we described *in vitro* was consistent with the reduced number of apoptotic cells observed specifically within the SEZ after the CC lesion. Also, we found not effects of PL in the differentiation potential of NSPCs. In conclusion, these results indicate that platelet-derived compounds promote NSPC survival and suggest that thrombocytes might contribute in CNS repair through a neuroprotective effect on SEZ-NSPCs that leads in increased cytogenic output of the SEZ. In the future it will be important to dissect further the identity of SEZ-NSPCs that are targeted by platelet-derived factors, whether these are NSCs, or downstream amplifying and more committed progenitors.

Platelets exert their functions both by cell-cell interactions and by paracrine activity mediated by released soluble factors. Although our *in vitro* work focused only on the effects of platelets' soluble compounds, our *in vivo* analysis indicates that cell-cell interactions might be also important in the platelet-NSPCs crosstalk. PL, as a source of microparticles and platelet-derived molecules, contains a plethora of growth factors and cytokines that might promote survival of NSPCs individually or cooperatively and it will be of great interest to identify those factors responsible for these effects (Hayon et al 2012b). PDGF is found in high concentrations in PL

(Nurden 2011) and rat derived NSPCs strongly express PDGFRα (Steffenhagen et al 2011). However, PDGF is a potent mitogen for CNS progenitors (Raff et al 1988) and we didn't observe any effects on cell proliferation. On the other hand, if anti-proliferative factors are also present in PL this might counteract the mitogenic effects of PDGF. Indeed, platelets contain and release high doses of TGF-β, a cytokine known to block NSPC proliferation *in vitro* and *in vivo* (Kandasamy et al 2010, Wachs et al 2006). Notably, TGF-β is also a potent neuroprotective cytokine (for review see (Aigner & Bogdahn 2008)); hence, it might be responsible for the enhanced survival and protection of NSPCs. Platelets also contain IGF-1 (Anitua et al 2013), VEGF and EGF (Nurden 2011). IGF-I has been shown to exert a powerful survival effect by inhibiting apoptotic cell death in PSA-NCAM+ adult NSPCs (Gago et al 2003). VEGF typically supports angiogenesis and has already been shown to be protective in adult NSPCs cultures and to support neuronal differentiation and survival (Schanzer et al 2004). EGF mainly promotes proliferation and migration of the transient amplifying pool of progenitors in the SEZ and their differentiation into oligodendrocytes (Gonzalez-Perez et al 2009). Finally, our data indicate that PL modulates the adhesive properties of NSPCs and we and others have previously shown that integrin-mediated adhesion is an important factor controlling the activation status and proliferative behavior of NSPCs (Kazanis et al 2010, Shen et al 2008).

The neurovascular unit (NVU) is increasingly recognized as a complex microenvironment composed of several cell types including neurons, astrocytes, oligodendrocytes, neural progenitors, microglia, endothelial cells, vascular smooth muscle cells, pericytes and blood-derived cells (Goldberg & Hirschi 2009, Lange et al 2013). The importance of both the cell-to-cell and the paracrine interactions between NSCs and endothelial cells was demonstrated by recent experimental work regarding the role of adhesion molecules and neurotrophin 3, respectively (Delgado et al 2014, Ottone et al 2014). We suggest that platelets are part of the rodent NVU, in particular after CNS damage. Apparently, as we have previously shown, the SEZ consists of a blood vessel network with distinct cytoarchitecture (Kazanis et al 2010) and is characterized by blood vessel fragments that are lacking tight junctions between endothelial cells as well as astrocytic endfeet and exhibits higher levels of leakage as compared to other areas of the brain (Tavazoie et al 2008). This might allow a more direct communication between the content of blood vessels and the SEZ parenchyma (Tavazoie et al 2008). In light of the above it

might not be surprising that platelets were present specifically in the vasculature of the ipsilateral SEZ in contrast to the ipsilateral non-cytogenic ventricular wall and the contralateral peri-ventricular zone after CC demyelination. There is always the possibility that platelets might actively migrate from the lesion site to the ventricular wall, or that they might reach the ventricular wall through the cerebral spinal fluid. However, the absence of platelet clusters at the non-cytogenic side of the ventricular wall, which is at equal distance from the lesion site as compared to the SEZ, favours the scenario of an active local recruitment of platelets through the blood circulation. Considering that animals were extensively perfused with saline before fixation, a manipulation that leads to the removal of all blood cells from the vessels, the accumulated platelets are most likely located in the extraluminal region. Nevertheless, a more detailed analysis is required to precisely identify the exact location of platelets in respect to the intra- and extra-luminal space of the ventricular wall vasculature, to assess their mechanism of migration and most importantly to define whether platelets exert their function in a direct cell-to-cell manner, via a paracrine function or through the mediation of a third cell-type such as endothelial cells or cells of the innate immune system.

It has been previously suggested that activated platelets as well as their microparticles contribute to recovery after brain injury (Hayon et al 2012a, Hayon et al 2012b). Indeed, in a recent paper (Hayon et al 2013) it was reported that the intracerebroventricular administration of platelet-rich plasma into an experimental model of stroke resulted in a significant increase in angiogenesis and in the number of proliferating SEZ-resident NSPCs. Although our experimental design is significantly different in terms of the injury model, the fact that we investigated the effects of PL on NSPCs *in vitro* and in that we studied directly the presence of platelets *in vivo*, the key conclusions are very consistent. In the rodent brain platelets seem to contribute to the enlargement of the pool of SEZ-resident NSPCs that are available for repair -via a range of mechanisms such as the enhancement of cell survival and/ or of cell proliferation- in a variety of CNS injuries. As platelets and platelet-derived lysates can be efficiently acquired by blood donations our results open a novel route that needs to be further explored in the context of the significantly different human brain in order to design strategies aiming at enhancing the cell generation capacity of endogenous neural stem cells in multiple pathologies such as stroke, demyelinating diseases or neuroinflammatory conditions.

Conflict of interests

Hereby, authors state that there is no conflict of interest with this study.

Acknowledgements

This work has been made possible through the support from the State Government of Salzburg (Austria), the German Federal Ministry of Education and Research (BMBF grant 01GN0978), the foundation Propter Homines (Liechtenstein), through funding from the European Union's Seventh Framework Program (FP7/2007-2013) under grant agreement n° HEALTH-F2-2011-278850 (INMiND) and n° HEALTH-F2-2011-279288 (IDEA), by a BBSRC UK grant (BB/I013210/1) to RJMF and IK as well as by the research funds from the Paracelsus Medical University PMU-FFF (Long-Term Fellowship to F.J.R. and Stand Alone grant) and the FWF Special Research Program (SFB) F44 "Cell Signaling in Chronic CNS Disorders". Moreover, we would like to acknowledge the microscopy core-facility (Mario Gimona) at the SCI-TReCS for technical support.

Reference

Aigner L, Bogdahn U. 2008. TGF-beta in neural stem cells and in tumors of the central nervous system. *Cell and tissue research* 331: 225-41

Alvarez-Buylla A, Garcia-Verdugo JM. 2002. Neurogenesis in adult subventricular zone. *The Journal of neuroscience : the official journal of the Society for Neuroscience* 22: 629-34

Anitua E, Zalduendo MM, Alkhraisat MH, Orive G. 2013. Release kinetics of platelet-derived and plasma-derived growth factors from autologous plasma rich in growth factors. *Annals of anatomy = Anatomischer Anzeiger : official organ of the Anatomische Gesellschaft* 195: 461-6

Brill A, Dashevsky O, Rivo J, Gozal Y, Varon D. 2005. Platelet-derived microparticles induce angiogenesis and stimulate post-ischemic revascularization. *Cardiovascular research* 67: 30-8

Carleton A, Petreanu LT, Lansford R, Alvarez-Buylla A, Lledo P-M. 2003. Becoming a new neuron in the adult olfactory bulb. *Nature neuroscience* 6: 507-18

Chen B, Sun HH, Wang HG, Kong H, Chen FM, Yu Q. 2012. The effects of human platelet lysate on dental pulp stem cells derived from impacted human third molars. *Biomaterials* 33: 5023-35

Culver JC, Vadakkan TJ, Dickinson ME. 2013. A specialized microvascular domain in the mouse neural stem cell niche. *PloS one* 8: e53546

Delgado AC, Ferron SR, Vicente D, Porlan E, Perez-Villalba A, et al. 2014. Endothelial NT-3 delivered by vasculature and CSF promotes quiescence of subependymal neural stem cells through nitric oxide induction. *Neuron* 83: 572-85

Deng W, Aimone JB, Gage FH. 2010. New neurons and new memories: how does adult hippocampal neurogenesis affect learning and memory? *Nature reviews. Neuroscience* 11: 339-50

Doetsch F, Scharff C. 2001. Challenges for Brain Repair: Insights from Adult Neurogenesis in Birds and Mammals. *Brain, Behavior and Evolution* 58: 306-22

Franklin RJ, Ffrench-Constant C. 2008. Remyelination in the CNS: from biology to therapy. *Nature reviews. Neuroscience* 9: 839-55
Franklin RJ, Kotter MR. 2008. The biology of CNS remyelination: the key to therapeutic advances. *J Neurol* 255 Suppl 1: 19-25
Gage FH. 2000. Mammalian Neural Stem Cells. *Science* 287: 1433-38
Gago N, Avellana-Adalid V, Baron-Van Evercooren A, Schumacher M. 2003. Control of cell survival and proliferation of postnatal PSA-NCAM(+) progenitors. *Molecular and cellular neurosciences* 22: 162-78
Goldberg JS, Hirschi KK. 2009. Diverse roles of the vasculature within the neural stem cell niche. *Regen Med* 4: 879-97
Gonzalez-Perez O, Romero-Rodriguez R, Soriano-Navarro M, Garcia-Verdugo JM, Alvarez-Buylla A. 2009. Epidermal growth factor induces the progeny of subventricular zone type B cells to migrate and differentiate into oligodendrocytes. *Stem Cells* 27: 2032-43
Hayon Y, Dashevsky O, Shai E, Brill A, Varon D, Leker RR. 2012a. Platelet microparticles induce angiogenesis and neurogenesis after cerebral ischemia. *Current neurovascular research* 9: 185-92
Hayon Y, Dashevsky O, Shai E, Varon D, Leker RR. 2013. Platelet lysates stimulate angiogenesis, neurogenesis and neuroprotection after stroke. *Thrombosis and haemostasis* 110: 323-30
Hayon Y, Shai E, Varon D, Leker RR. 2012b. The role of platelets and their microparticles in rehabilitation of ischemic brain tissue. *CNS & neurological disorders drug targets* 11: 921-5
Horstman LL, Jy W, Ahn YS, Zivadinov R, Maghzi AH, et al. 2010. Role of platelets in neuroinflammation: a wide-angle perspective. *Journal of neuroinflammation* 7: 10
Hunt J, Cheng A, Hoyles A, Jervis E, Morshead CM. 2010. Cyclosporin A has direct effects on adult neural precursor cells. *The Journal of neuroscience : the official journal of the Society for Neuroscience* 30: 2888-96
Kandasamy M, Couillard-Despres S, Raber KA, Stephan M, Lehner B, et al. 2010. Stem cell quiescence in the hippocampal neurogenic niche is associated with elevated transforming growth factor-beta signaling in an animal model of Huntington disease. *Journal of neuropathology and experimental neurology* 69: 717-28
Kaushansky K. 2006. Lineage-specific hematopoietic growth factors. *The New England journal of medicine* 354: 2034-45
Kazanis I. 2013. Neurogenesis in the adult mammalian brain: how much do we need, how much do we have? *Current topics in behavioral neurosciences* 15: 3-29
Kazanis I, Gorenkova N, Zhao JW, Franklin RJ, Modo M, Ffrench-Constant C. 2013. The late response of rat subependymal zone stem and progenitor cells to stroke is restricted to directly affected areas of their niche. *Experimental neurology* 248: 387-97
Kazanis I, Lathia JD, Vadakkan TJ, Raborn E, Wan R, et al. 2010. Quiescence and activation of stem and precursor cell populations in the subependymal zone of the mammalian brain are associated with distinct cellular and extracellular matrix signals. *The Journal of neuroscience : the official journal of the Society for Neuroscience* 30: 9771-81
Lange S, Trost A, Tempfer H, Bauer HC, Bauer H, et al. 2013. Brain pericyte plasticity as a potential drug target in CNS repair. *Drug discovery today* 18: 456-63
Langer HF, Chavakis T. 2013. Platelets and neurovascular inflammation. *Thrombosis and haemostasis* 110
Langer HF, Choi EY, Zhou H, Schleicher R, Chung KJ, et al. 2012. Platelets contribute to the pathogenesis of experimental autoimmune encephalomyelitis. *Circulation research* 110: 1202-10
Levine JM, Reynolds R, Fawcett JW. 2001. The oligodendrocyte precursor cell in health and disease. *Trends Neurosci* 24: 39-47
Li Z, Burns AR, Han L, Rumbaut RE, Smith CW. 2011. IL-17 and VEGF are necessary for efficient corneal nerve regeneration. *The American journal of pathology* 178: 1106-16
Lohmann M, Walenda G, Hemeda H, Joussen S, Drescher W, et al. 2012. Donor age of human platelet lysate affects proliferation and differentiation of mesenchymal stem cells. *PloS one* 7: e37839
Lois C, Garcia-Verdugo JM, Alvarez-Buylla A. 1996. Chain migration of neuronal precursors. *Science* 271: 978-81
Menn B, Garcia-Verdugo JM, Yaschine C, Gonzalez-Perez O, Rowitch D, Alvarez-Buylla A. 2006. Origin of oligodendrocytes in the subventricular zone of the adult brain. *The Journal of neuroscience : the official journal of the Society for Neuroscience* 26: 7907-18
Michelson AD. 2010. Antiplatelet therapies for the treatment of cardiovascular disease. *Nature reviews. Drug discovery* 9: 154-69
Morshead CM, van der Kooy D. 1992. Postmitotic death is the fate of constitutively proliferating cells in the subependymal layer of the adult mouse brain. *The Journal of neuroscience : the official journal of the Society for Neuroscience* 12: 249-56

Nait-Oumesmar B, Decker L, Lachapelle F, Avellana-Adalid V, Bachelin C, Van Evercooren AB. 1999. Progenitor cells of the adult mouse subventricular zone proliferate, migrate and differentiate into oligodendrocytes after demyelination. *The European journal of neuroscience* 11: 4357-66

Nurden AT. 2011. Platelets, inflammation and tissue regeneration. *Thrombosis and haemostasis* 105 Suppl 1: S13-33

Ottone C, Krusche B, Whitby A, Clements M, Quadrato G, et al. 2014. Direct cell-cell contact with the vascular niche maintains quiescent neural stem cells. *Nature cell biology* 16: 1045-56

Picard-Riera N, Decker L, Delarasse C, Goude K, Nait-Oumesmar B, et al. 2002. Experimental autoimmune encephalomyelitis mobilizes neural progenitors from the subventricular zone to undergo oligodendrogenesis in adult mice. *Proc Natl Acad Sci U S A* 99: 13211-6

Raff MC, Lillien LE, Richardson WD, Burne JF, Noble MD. 1988. Platelet-derived growth factor from astrocytes drives the clock that times oligodendrocyte development in culture. *Nature* 333: 562 - 65

Rivera FJ, Couillard-Despres S, Pedre X, Ploetz S, Caioni M, et al. 2006. Mesenchymal Stem Cells Instruct Oligodendrogenic Fate Decision on Adult Neural Stem Cells. *STEM CELLS* 24: 2209-19

Sandner B, Rivera FJ, Caioni M, Nicholson L, Eckstein V, et al. 2013. Bone morphogenetic proteins prevent bone marrow stromal cell-mediated oligodendroglial differentiation of transplanted adult neural progenitor cells in the injured spinal cord. *Stem cell research* 11: 758-71

Schallmoser K, Bartmann C, Rohde E, Reinisch A, Kashofer K, et al. 2007. Human platelet lysate can replace fetal bovine serum for clinical-scale expansion of functional mesenchymal stromal cells. *Transfusion* 47: 1436-46

Schallmoser K, Strunk D. 2009. Preparation of pooled human platelet lysate (pHPL) as an efficient supplement for animal serum-free human stem cell cultures. *Journal of visualized experiments : JoVE*

Schallmoser K, Strunk D. 2013. Generation of a pool of human platelet lysate and efficient use in cell culture. *Methods in molecular biology* 946: 349-62

Schanzer A, Wachs FP, Wilhelm D, Acker T, Cooper-Kuhn C, et al. 2004. Direct stimulation of adult neural stem cells in vitro and neurogenesis in vivo by vascular endothelial growth factor. *Brain pathology* 14: 237-48

Semple JW, Italiano JE, Jr., Freedman J. 2011. Platelets and the immune continuum. *Nature reviews. Immunology* 11: 264-74

Shen Q, Wang Y, Kokovay E, Lin G, Chuang SM, et al. 2008. Adult SVZ stem cells lie in a vascular niche: a quantitative analysis of niche cell-cell interactions. *Cell Stem Cell* 3: 289-300

Sotnikov I, Veremeyko T, Starossom SC, Barteneva N, Weiner HL, Ponomarev ED. 2013. Platelets recognize brain-specific glycolipid structures, respond to neurovascular damage and promote neuroinflammation. *PloS one* 8: e58979

Steffenhagen C, Dechant FX, Oberbauer E, Furtner T, Weidner N, et al. 2012. Mesenchymal Stem Cells Prime Proliferating Adult Neural Progenitors Towards An Oligodendrocyte Fate. *Stem Cells Dev*

Steffenhagen C, Kraus S, Dechant FX, Kandasamy M, Lehner B, et al. 2011. Identity, fate and potential of cells grown as neurospheres: species matters. *Stem Cell Rev* 7: 815-35

Steinman L. 2012. Platelets provide a bounty of potential targets for therapy in multiple sclerosis. *Circulation research* 110: 1157-8

Tavazoie M, Van der Veken L, Silva-Vargas V, Louissaint M, Colonna L, et al. 2008. A specialized vascular niche for adult neural stem cells. *Cell Stem Cell* 3: 279-88

Thored P, Wood J, Arvidsson A, Cammenga J, Kokaia Z, Lindvall O. 2007. Long-term neuroblast migration along blood vessels in an area with transient angiogenesis and increased vascularization after stroke. *Stroke; a journal of cerebral circulation* 38: 3032-9

Vandesompele J, De Preter K, Pattyn F, Poppe B, Van Roy N, et al. 2002. Accurate normalization of real-time quantitative RT-PCR data by geometric averaging of multiple internal control genes. *Genome biology* 3: RESEARCH0034

Wachs FP, Winner B, Couillard-Despres S, Schiller T, Aigner R, et al. 2006. Transforming growth factor-beta1 is a negative modulator of adult neurogenesis. *Journal of neuropathology and experimental neurology* 65: 358-70

Warnke PH, Humpe A, Strunk D, Stephens S, Warnke F, et al. 2013. A clinically-feasible protocol for using human platelet lysate and mesenchymal stem cells in regenerative therapies. *Journal of cranio-maxillo-facial surgery : official publication of the European Association for Cranio-Maxillo-Facial Surgery* 41: 153-61

Woodruff RH, Franklin RJ. 1999. Demyelination and remyelination of the caudal cerebellar peduncle of adult rats following stereotaxic injections of lysolecithin, ethidium bromide, and complement/anti-galactocerebroside: a comparative study. *Glia* 25: 216-28

Figure legends

Figure 1: LV and SEZ cellular response to CC lesion: increased laminin expression and cell density. (A) Schematic diagram of a coronal section of the brain, showing the site of lesion in the CC (in brown) and the four areas in which quantifications were performed: the SEZ and the medial ventricular wall ipsilateral to the lesion (in red and green, respectively), as well as the SEZ and medial wall contralateral to the lesion (in blue and yellow, respectively). (B) Illustration of a typical example of immunostaining for laminin (in red) in a coronal section taken from a mouse brain depicting the method of quantification of blood vessel (b.v.) density. The area extending up to 20 μm from the ventricular wall (that contains the SEZ) was delineated as shown with the white interrupted line. Within this area, the length of all laminin+ vessels was measured (cyan lines). (C) Quantification of laminin-expressing b.v. after normalization per length of the ventricular wall and expressed as changes in respect to the contralateral (unaffected) SEZ per time-point. Note that no changes were found between areas at 4 dpl, while both at 7 and 15 dpl the expression of laminin was significantly increased in the SEZ and in the medial wall ipsilateral to the lesion (white and white-striped bars) indicating a stress response of the vasculature at both areas. Significant changes between the same areas compared with 4 dpl are indicated by one "#" (a significant interaction between time and area was found with $F=3.331$ and $P=0.007$). Significant changes between different areas and the SEZ contra are indicated by *** (The effect of the area was found to be significant with $F=29.76$ and, $P<0.0001$). Statistical analysis was performed using a two-way ANOVA, followed by the Sidak's post-hoc test. (D, E) High magnifications of the SEZ after immunostaining for Ki67 (to label proliferating cells, in green) and nestin (to mark NSPC, in red) in control mice and in mice sacrificed at 7 days post the lysolecithin-induced lesion. (F) Graph showing the density of cells within the SEZ contralateral (black bars) and ipsilateral (grey bars) to the lesion, at 4 and 7 days post-lesion. Note the significant increase in cell density at both time-points. (G) Graph showing the density of proliferating (Ki67+) cells within the SEZ contralateral (black bars) and ipsilateral (grey bars) to the lesion, at 4 and 7 days post-lesion. Note the significant increase in the density of mitotic cells at both time-points. In both graphs cell density was calculated as number of cells per length of the ventricular wall. [*: $p<0.05$ using a two-way ANOVA, followed by the Sidak's post-hoc test. Scale bar: 75μm]

Figure 2: Lack of activation of the SEZ in response to mechanical injury in the CC. (A-C) Distribution of platelets and laminin-expressing vessels 7days post-injection of (A) lysolecithin, (B) vehicle and (C) in the contralateral (non-injected) hemisphere. Low magnification photographs of coronal brain sections immunostained for laminin (marking blood vessels, in red) and CD41 (marking platelets, in green). Injection of lysolecithin in the CC (A) results in a focal lesion (indicated by the star) and in the increase of laminin expression on blood vessels both within the area of lesion and in the periventricular tissue (compare with non-injected hemisphere shown in C). Notably, CD41+ platelets accumulate in blood vessels within the lesion and the SEZ cytogenic niche (indicated by white arrows and blown up in the inset). However, injection of vehicle (B) results in the focal disruption of the CC tissue (star) and by increased expression of laminin on blood vessels, but without inducing the expression of laminin and the accumulation of platelets within the neighbouring SEZ. (D) Graphs showing the absence of a cytogenic response in the ipsilateral compared to the contralateral SEZ after the injection of vehicle in the CC, as judged by the lack of change both in the overall number of cells in the niche (at the left) and in the density of Ki67+ cells (at the right). [Scale bar: 100μm; note that in A,B the SEZ is at the left side of the image, whilst in C the SEZ is at the right side of the image.]

Figure 3: Platelets' periventricular distribution after lysolecithin-induced demyelination in the CC. Low magnification images of the contralateral (A) and the lesioned (B) lateral ventricles (LV), 4 days after the injection of lysolecithin (1%, 2 μl) in the supraventricular CC. Although no platelet accumulation is detected around the contralateral (unaffected) LV, numerous blood vessels (immunostained with laminin, in red) appear to contain CD41+ platelets (in green, indicated by white arrowheads) at the affected hemisphere. Notably, platelets are found in vessels positioned specifically adjacent to the lateral wall of the LV (towards the right in B), where the SEZ cytogenic stem cell niche is located, and not at the medial, non-cytogenic side, or deeper into the striatum. (C) Graph showing the quantification of the fraction of laminin-expressing blood vessels (b.v.) where CD41+ platelets were detected at different time-points post-lesion. Note the specific and significant increase in the presence of platelets within b.v. of the SEZ at all time-points. Statistical analysis was performed with a two-way ANOVA, followed by the Dunnett's post-hoc test per each time-point (indicated by ***: $F=76.34$; $P<0.0001$). (D) Epifluorescence images showing CD41+ platelets (in green), nestin+ NSPCs (in red) and Ki-67+

proliferating cells (in white) within the SEZ ipsilateral to the lesion. Notice the proximity of platelet clusters to proliferating NSPCs indicated by yellow arrowheads. [Scale bars: 150 μm]

Figure 4: Micro-anatomy of platelets and blood vessels. (A) Higher magnification of the boxed area indicated in Figure 3B1 showing two blood vessels in which CD41+ platelets have accumulated. Importantly, numerous CD41+ platelets are also found outside blood vessels, in the parenchyma, specifically at the site of the lesion in the CC (over the dorsal wall of the LV) and not within the cytogenic niche (at the lateral wall). (B) High magnification of a laminin+ blood vessel located in the contralateral SEZ (indicated by a thin yellow arrow in Figure 3A2) with no CD41+ platelets. (C) High magnification of a laminin+ blood vessel located in the ipsilateral, lesioned CC (the vessel boxed in A3). Note the presence of multiple CD41+ platelets both inside and outside the vessel. (D) High magnification of a laminin+ blood vessel located in the ipsilateral SEZ (indicated by a thick yellow arrow in Figure 3B1) with multiple CD41+ platelets. (E-G) High magnifications of transverse sections of laminin+ blood vessels showing the presence of CD41 immunopositive particles in different domains: attached to the walls of the vessels, towards the lumen of the vessel (in G) or migrating away (in E, indicated by white arrowheads). [scale bars: 20 μm in A; 5 μm in B-D, 10 μm in E-G]

Figure 5: PL promotes adherence and expansion of proliferating NSPCs. Phase contrast images show the morphology of NSPCs incubated in normal proliferating medium (control) (A, B, C), supplemented with 1% PL (D, E, F), 5% PL (G, H, I) or 10% PL (J, K, L). Images show NSPCs during proliferation on day 1 (A, D, G, J), day 3 (B, E, H, K) and day 7 (C, F, I, L). Note that under PL conditions NSPCs attached to the surface, while in the control the cells grew as floating neurospheres. Scale bar = 50 μm. The cell number was determined with the CASY cell counter (M) and the Trypan blue exclusion (N) over a period of 7 days during proliferation. The data were normalized to the control. Cell number significantly increased in the presence of PL in a dose dependent manner. All experiments were performed in triplicates and three independent experiments were considered for statistical analysis. Data are shown as mean +/- SD. For statistical analysis two-way ANOVA-Bonferroni post-hoc was performed. *** = $p < 0.001$.

Figure 6: PL does not affect the cell intrinsic fate of NSPCs. The marker expression profile and the cell identity of different proliferating NSPCs subpopulations were analyzed by immunofluorescence and RT-PCR. The cells were dissociated and seeded on coated coverslip overnight and processed for staining. Fluorescence images show an overview of the markers A2B5 (A, B, C, D); NG2 (E, F, G, H) and Olig2 (I, J, K, L). Scale bar = 100 µm (A-H) and (I-L). Considering that very few NPSCs express DCX, higher magnification fluorescent images illustrate typical DCX-expressing cells in all conditions (M, N, O, P). Scale bar = 50 µm. Quantitative analysis revealed no significant difference in the expression of A2B5 (Q), NG2 (R), Olig2 (S) and DCX (T). No change was observed in all markers upon PL exposure. The RT-PCR data show that PL does not affect the expression of cell fate determinants such as Id2 (U) and Olig2 (V) as well as the neuronal precursor marker DCX (W). Data are shown as mean +/- SD. For statistical analysis One-way ANOVA was performed.

Figure 7: PL does not affect the differentiation potential of proliferating NSPCs. The pretreated proliferating NSPCs were dissociated and cultivated in the absence of growth factors for 7 days and staining for different cell-lineage markers was performed. Thus, the response to growth factor withdrawal was analyzed. No significant differences were observed in the expression of CNP (B), GalC (D), MBP (F), GFAP (H), Beta3-Tubulin (J) and Map2a+2b (L). Representative fluorescence images of the markers CNP (A), GalC (C), MBP (E), GFAP (G), Beta3-Tubulin (I) and Map2a+2b (K) are shown. Scale bar = 100 µm (A-G); Scale bar = 50 µm (I-K). Data are shown as mean +/- SD. For statistical analysis One-way ANOVA-Tukey post-hoc was performed.

Figure 8: PL does not influence the cell cycle of NSPCs. The cells were treated with the control medium alone, or supplemented with 1%, 5% or 10% PL. The G0/G1 (A) and G2/S/M phases (B) were analyzed by flow cytometry using propidium iodide. Three different time points (day 0, 4 and 7) were chosen for the analysis. No differences were found in the proportion of

cells in G0/G1 (A) and in G2/S/M phase (B) in the different cultures. Data are shown as mean +/- SD. Two-way ANOVA Bonferroni post-hoc was performed for statistical analysis.

Figure 9: PL increases cell viability and protects NSPCs from apoptosis. The cells were exposed to different media under proliferating conditions: control, 1% PL, 5% or 10%. Different assays were used to determine the cell viability during proliferation. Cell viability was evaluated by CASY cell counter (A) and Trypan blue exclusion (B). Note the increased viability of PL-treated cells. The percentage of apoptotic cells was quantified by flow cytometry using propidium iodide (C). The proportion of apoptotic cells decreased after 4 days 1% and 5% PL exposure. To validate the apoptosis data by an independent method, TUNEL assay was performed (D). The TUNEL assay results also indicate an anti-apoptotic effect of PL. Data are shown as mean +/- SD. For statistical analysis one-way ANOVA-Tukey post-hoc and two-way ANOVA-Bonferroni post-hoc was performed. * = $p < 0.05$; ** = $p < 0.01$; *** = $p < 0.001$. **Increased occurrence of apoptotic cells in the medial (non-cytogenic) wall of the LV after a lesion in the CC.** (E, F) Microphotographs from coronal mouse brain sections taken from tissue at 4dpl and immunostained for caspase 3 (in green) showing the medial (in E) and the lateral (in F) LV wall. Note the decreased numbers of caspase 3+ cells at the SEZ, cytogenic lateral wall when compared to the medial non-cytogenic wall). (G) Graph showing the quantification of the density of caspase 3+ cells at the medial and lateral LV walls of the ipsilateral to the lesion hemisphere. [*: $p<0.05$, using t test analysis; scale bar for A, B: 5-μm].

Figure 10: Reduced levels of apoptosis within the SEZ ipsilateral to demyelination. (panels A-D) High magnification images of mouse brain sections immunostained for activated caspase 3 (in green) and nestin (in red). Numerous double casp3+nestin+ cells are detected within the contralateral (unaffected) SEZ, both dorsally (A) and in the middle (C). The number of casp3+ cells is decreased in the SEZ ipsilateral to the lesion at 4dpl, both dorsally (B) and in the middle (D). The illustration in E shows in boxes the areas that were investigated and depicted in panels A-D. (F) Graph showing the significant increase in the fraction of nestin+ NSPCs within the ipsilateral SEZ in response to demyelination (4dpl). (G) Graph showing the significant decrease in the overall fraction of apoptotic cells within the ipsilateral SEZ at 4dpl. (H) Graph showing the

significant decrease in the fraction of nestin+ NSCPs that co-express caspase3 (are apoptotic) within the ipsilateral SEZ at 4dpl. [*: $p<0.05$, paired t-test analysis]

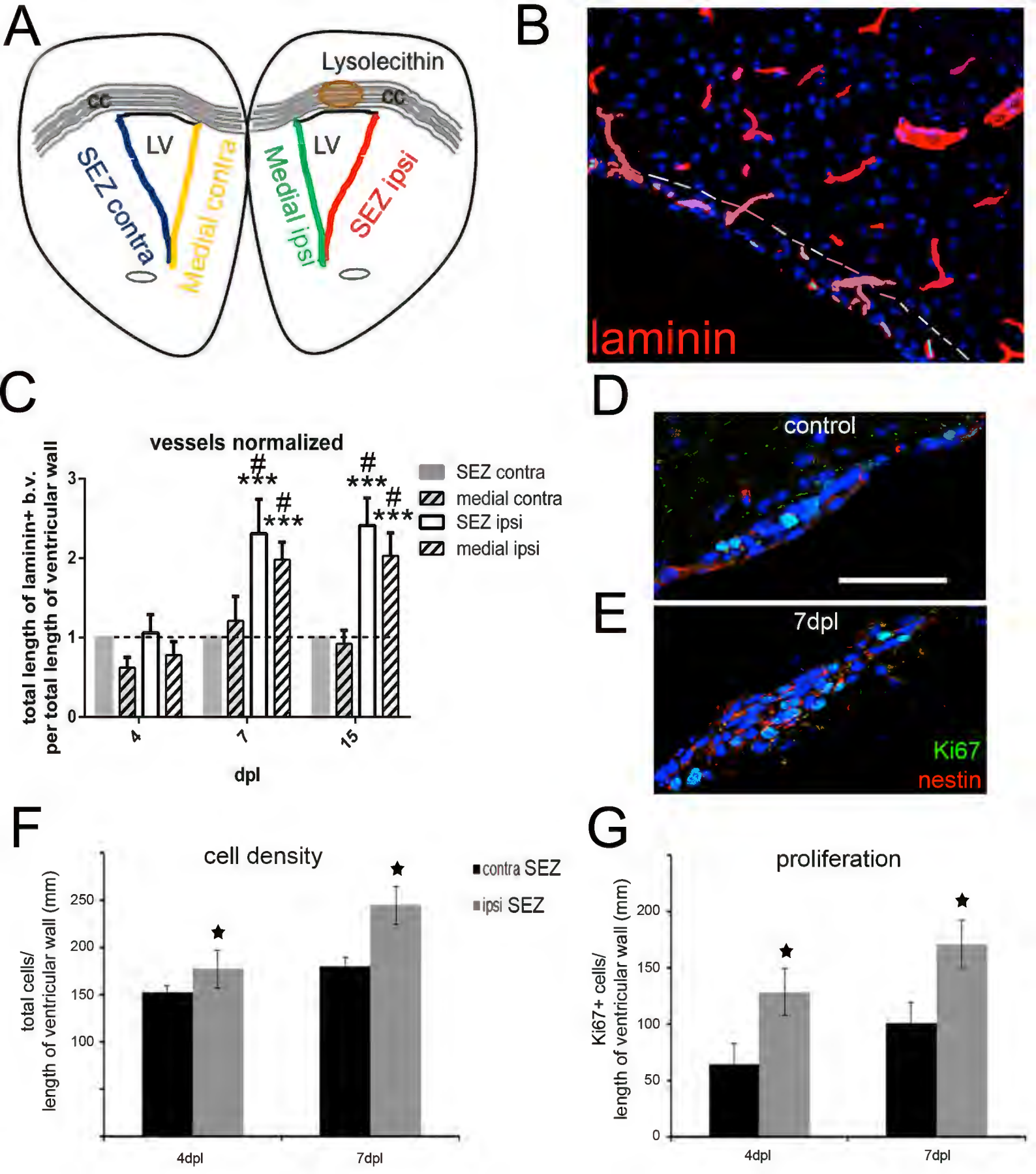
A
Lysolecithin
CC
CC
LV
LV
SEZ contra
Medial contra
Medial ipsi
SEZ ipsi
B
laminin
C
vessels normalized
total length of laminin+ b.v.
per total length of ventricular wall
SEZ contra
medial contra
SEZ ipsi
medial ipsi
dpl
D
control
E
7dpl
Ki67
nestin
F
cell density
total cells/
length of ventricular wall (mm)
contra SEZ
ipsi SEZ
4dpl
7dpl
G
proliferation
Ki67+ cells/
length of ventricular wall (mm)
4dpl
7dpl

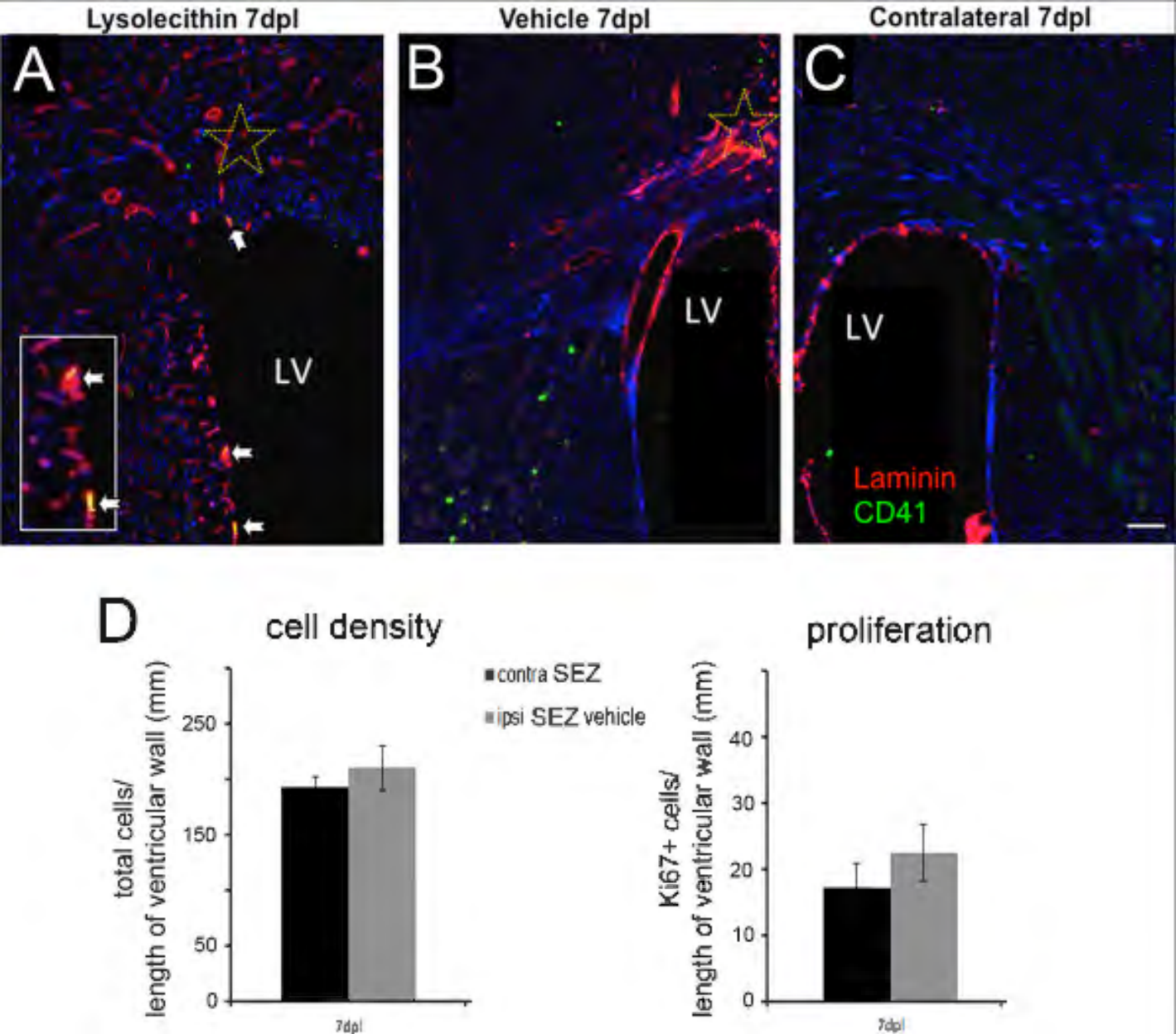
Lysolecithin 7dpl
Vehicle 7dpl
Contralateral 7dpl
A
B
C
LV
LV
LV
Laminin
CD41
D
cell density
proliferation
contra SEZ
ipsi SEZ vehicle
total cells/
length of ventricular wall (mm)
250
150
50
0
7dpl
Ki67+ cells/
length of ventricular wall (mm)
40
30
20
10
0
7dpl

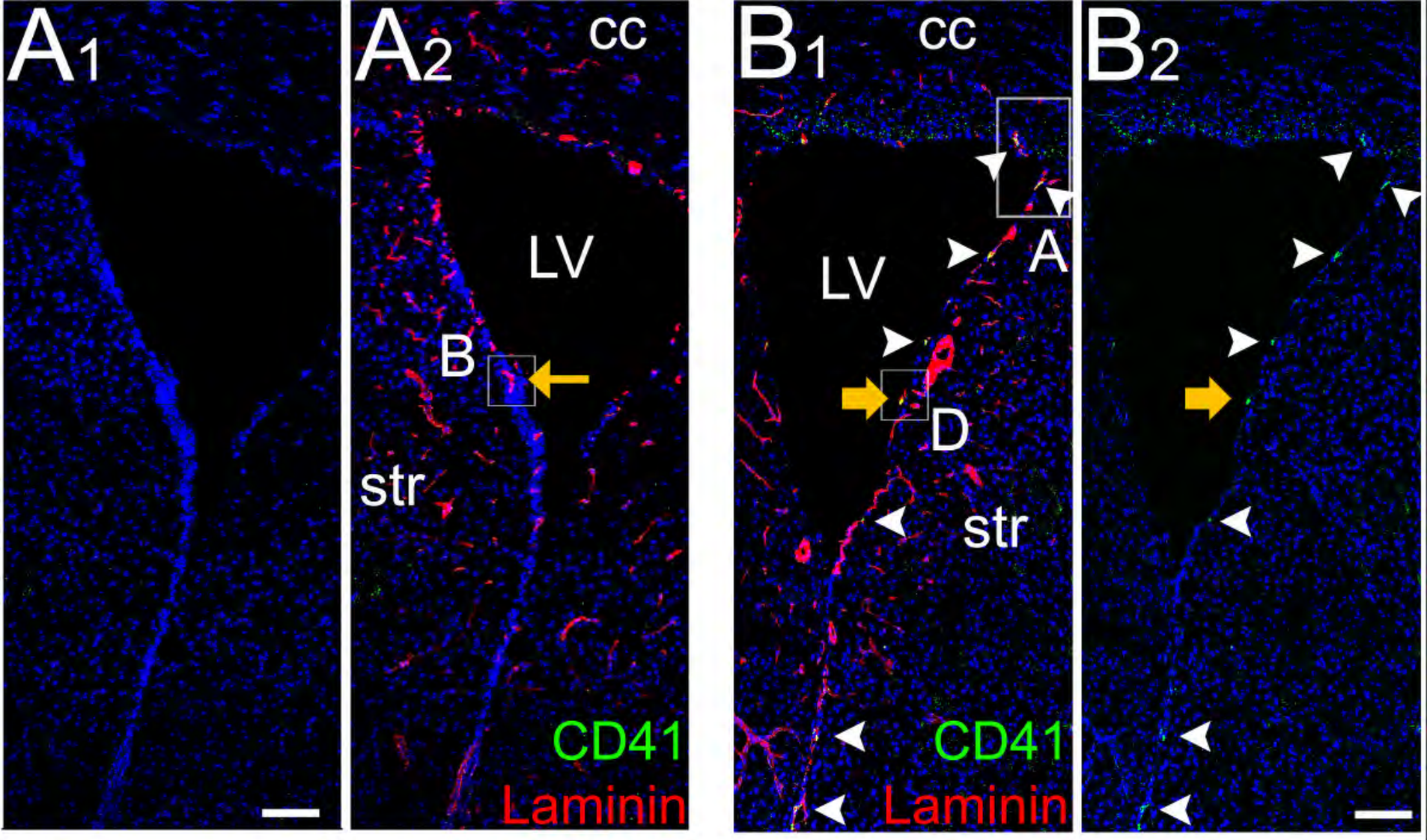
A1
A2
cc
LV
B
str
CD41
Laminin
B1
cc
LV
A
D
str
CD41
Laminin
B2

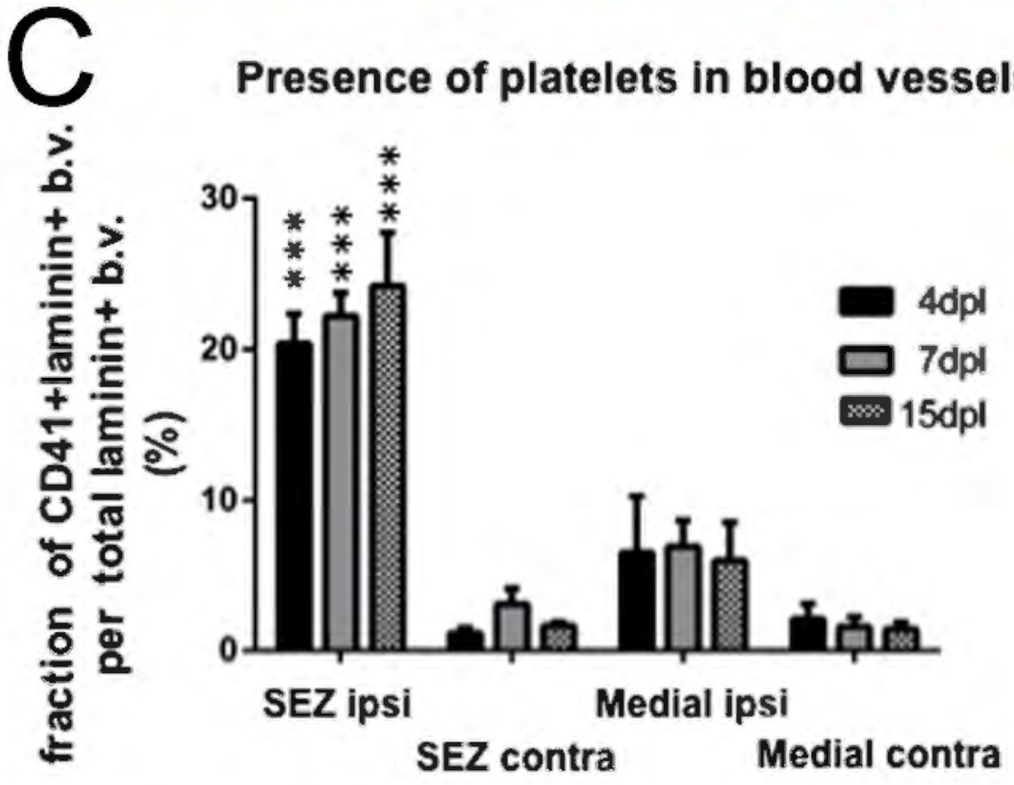
C
Presence of platelets in blood vessels
fraction of CD41+laminin+ b.v. per total laminin+ b.v. (%)
30
20
10
0
***
***
***
4dpl
7dpl
15dpl
SEZ ipsi
SEZ contra
Medial ipsi
Medial contra

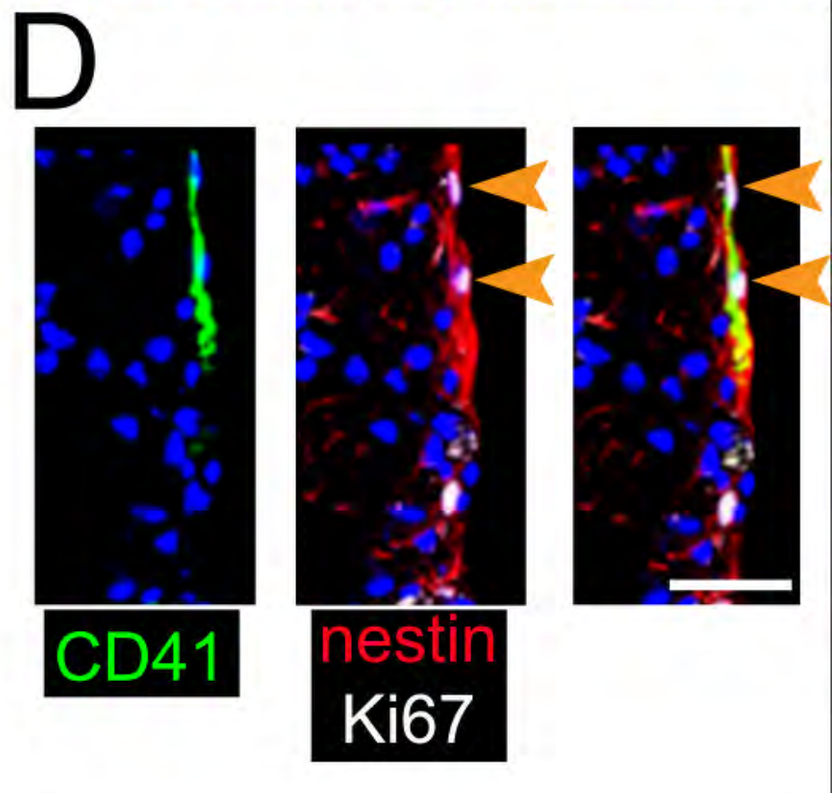
D
CD41
nestin
Ki67

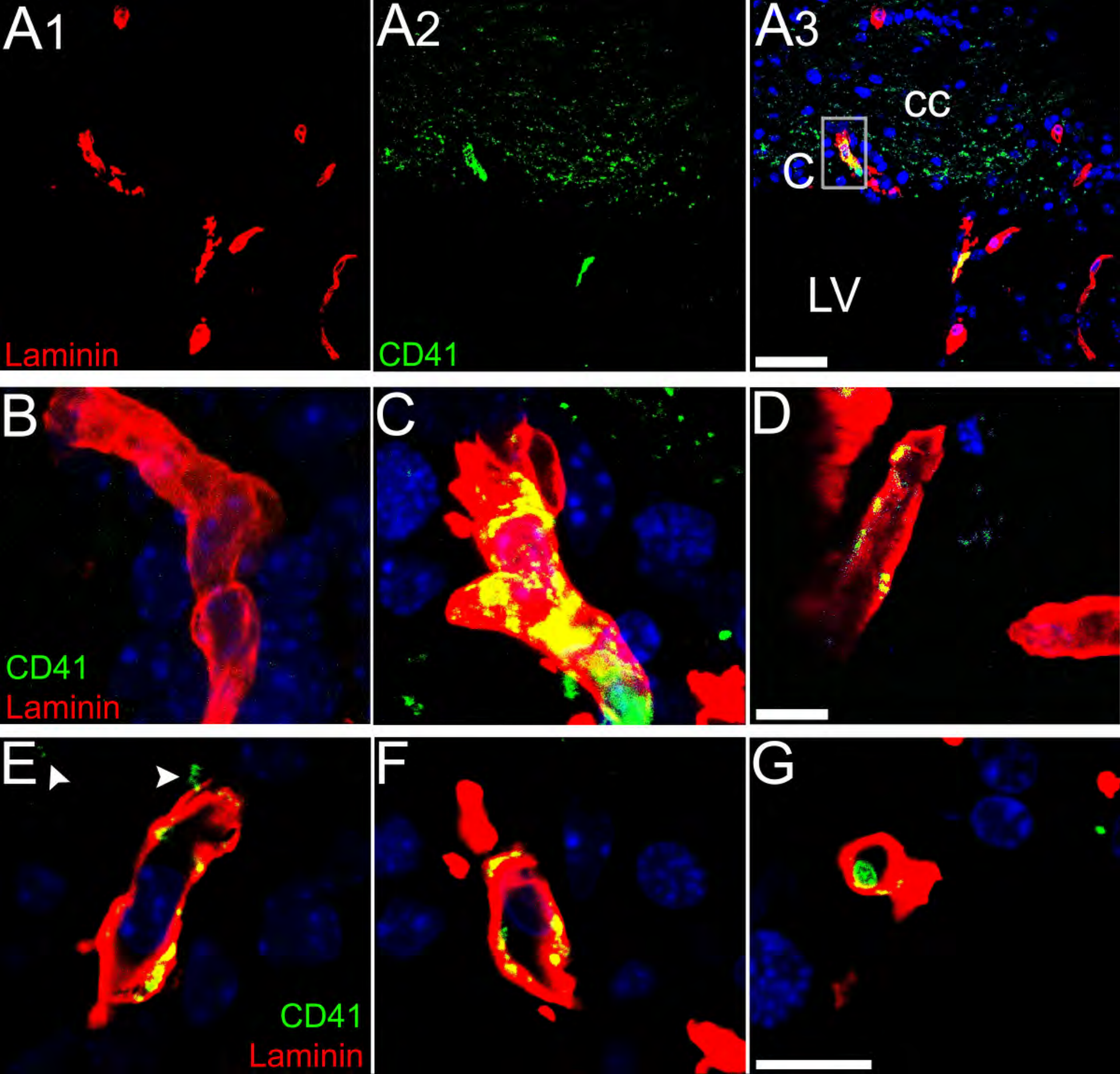
A1
Laminin
A2
CD41
A3
cc
C
LV
B
CD41
Laminin
C
D
E
CD41
Laminin
F
G

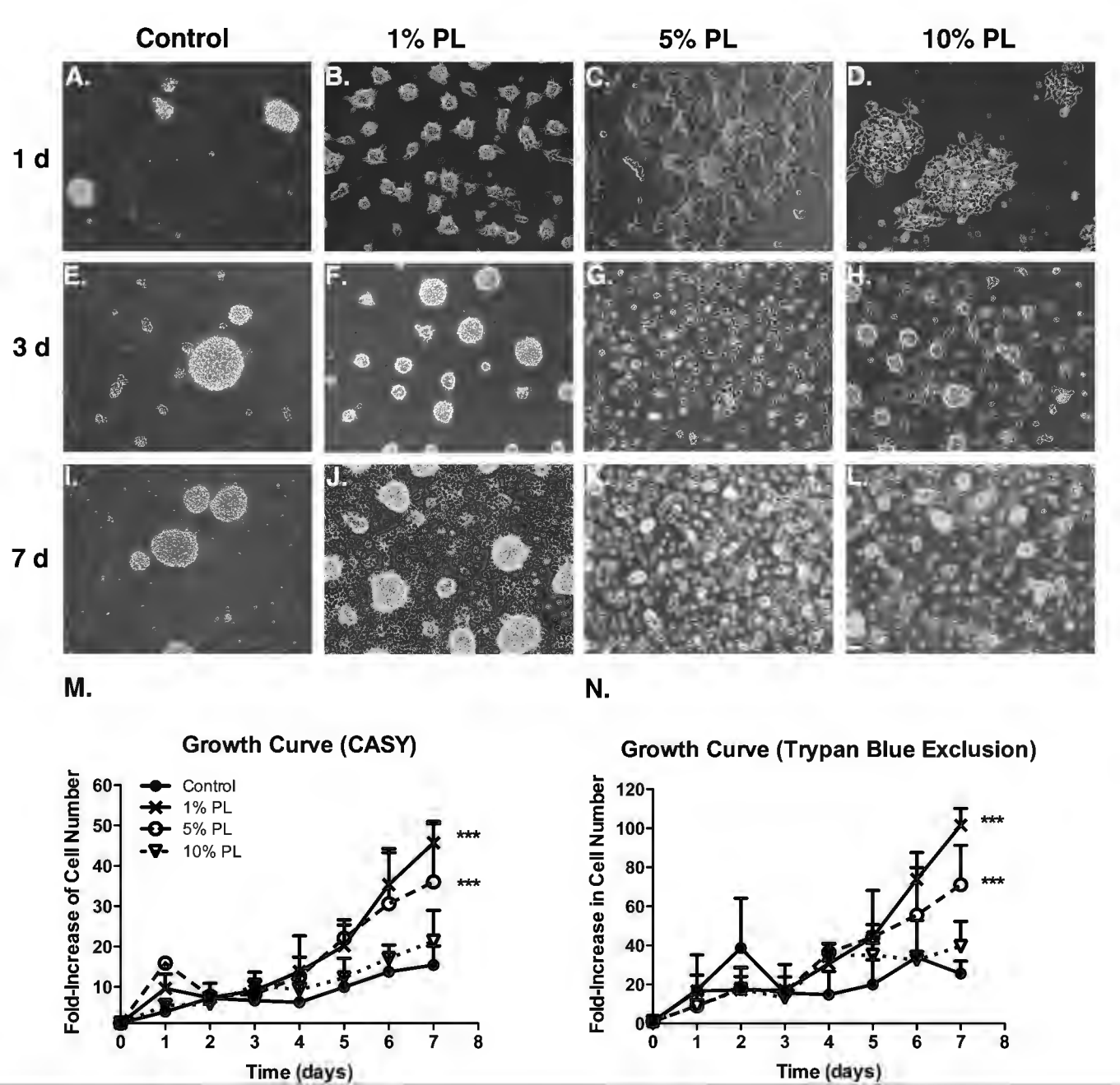
Control
1% PL
5% PL
10% PL
1 d
3 d
7 d
A.
B.
C.
D.
E.
F.
G.
H.
I.
J.
K.
L.
M.
N.
Growth Curve (CASY)
Fold-Increase of Cell Number
Time (days)
Control
1% PL
5% PL
10% PL
***
***
Growth Curve (Trypan Blue Exclusion)
Fold-Increase in Cell Number
Time (days)
***
***

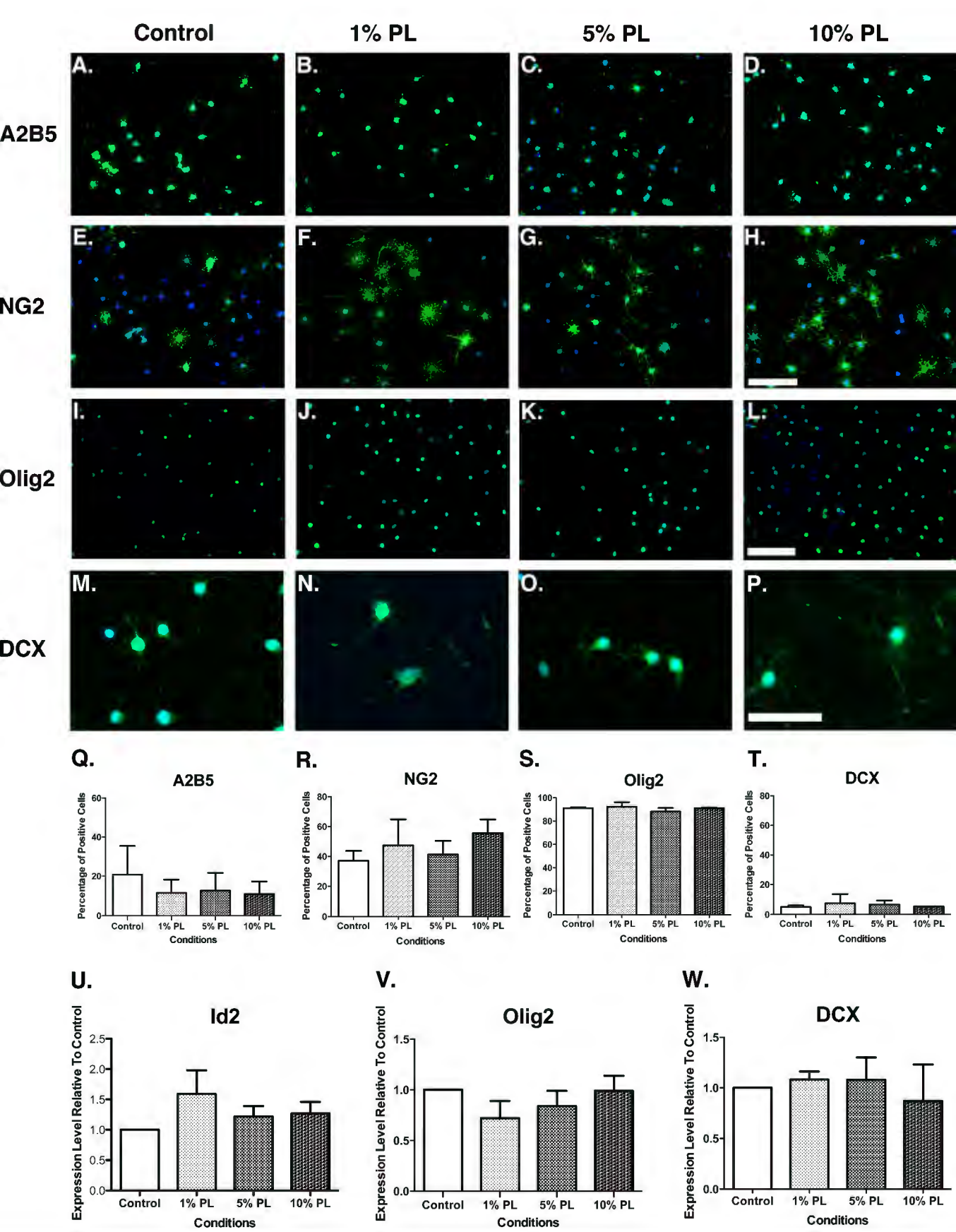
Control
1% PL
5% PL
10% PL
A2B5
NG2
Olig2
DCX
A.
B.
C.
D.
E.
F.
G.
H.
I.
J.
K.
L.
M.
N.
O.
P.
Q.
A2B5
R.
NG2
S.
Olig2
T.
DCX
Percentage of Positive Cells
Control
1% PL
5% PL
10% PL
Conditions
U.
Id2
V.
Olig2
W.
DCX
Expression Level Relative To Control

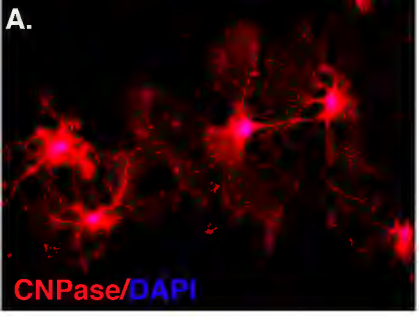
A.
CNPase/DAPI

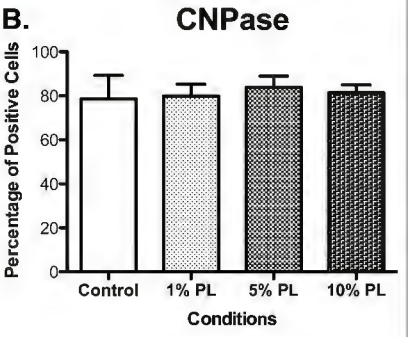
B.
CNPase
Percentage of Positive Cells
100
80
60
40
20
0
Control
1% PL
5% PL
10% PL
Conditions

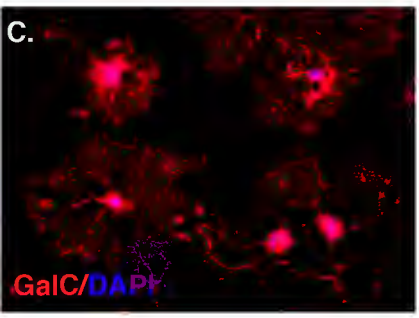
C.
GalC/DAPI

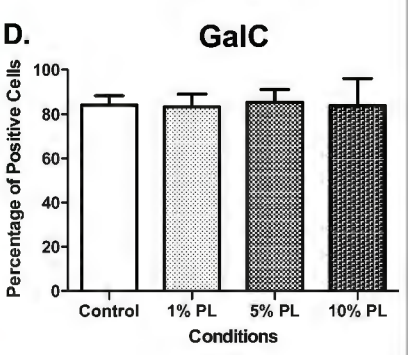
D.
GalC
Percentage of Positive Cells
100
80
60
40
20
0
Control
1% PL
5% PL
10% PL
Conditions

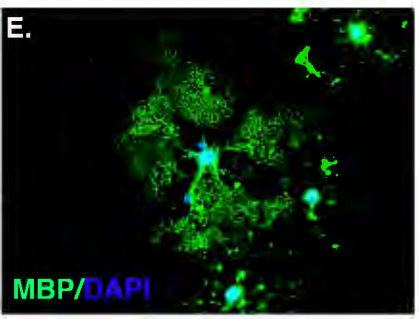
E.
MBP/DAPI

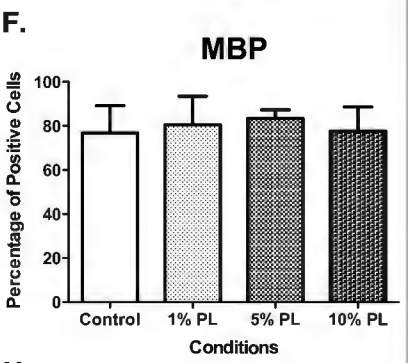
F.
MBP
Percentage of Positive Cells
100
80
60
40
20
0
Control
1% PL
5% PL
10% PL
Conditions

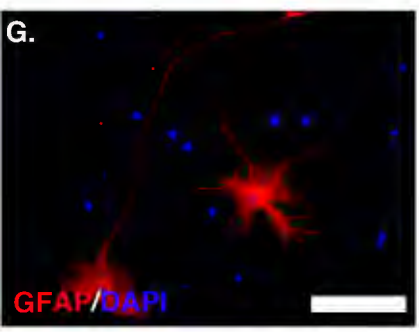
G.
GFAP/DAPI

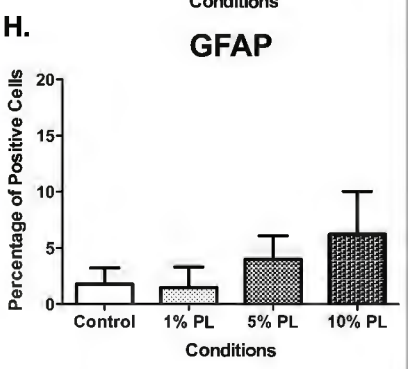
H.
GFAP
Percentage of Positive Cells
20
15
10
5
0
Control
1% PL
5% PL
10% PL
Conditions

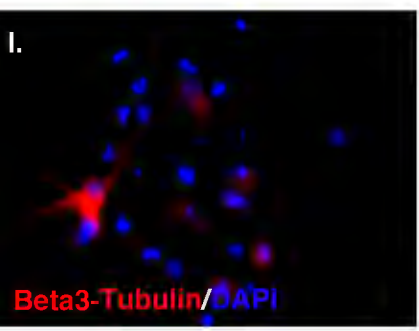
I.
Beta3-Tubulin/DAPI

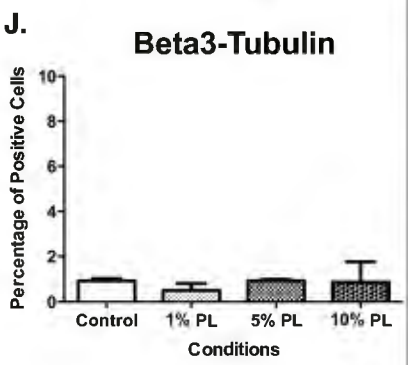
J.
Beta3-Tubulin
Percentage of Positive Cells
10
8
6
4
2
0
Control
1% PL
5% PL
10% PL
Conditions

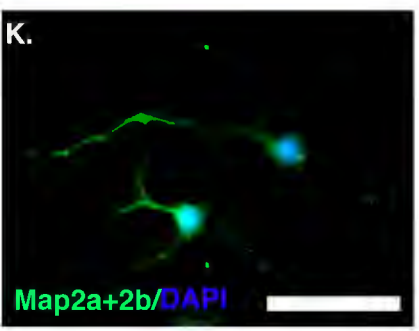
K.
Map2a+2b/DAPI

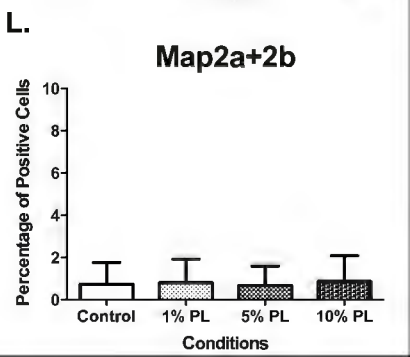
L.
Map2a+2b
Percentage of Positive Cells
10
8
6
4
2
0
Control
1% PL
5% PL
10% PL
Conditions

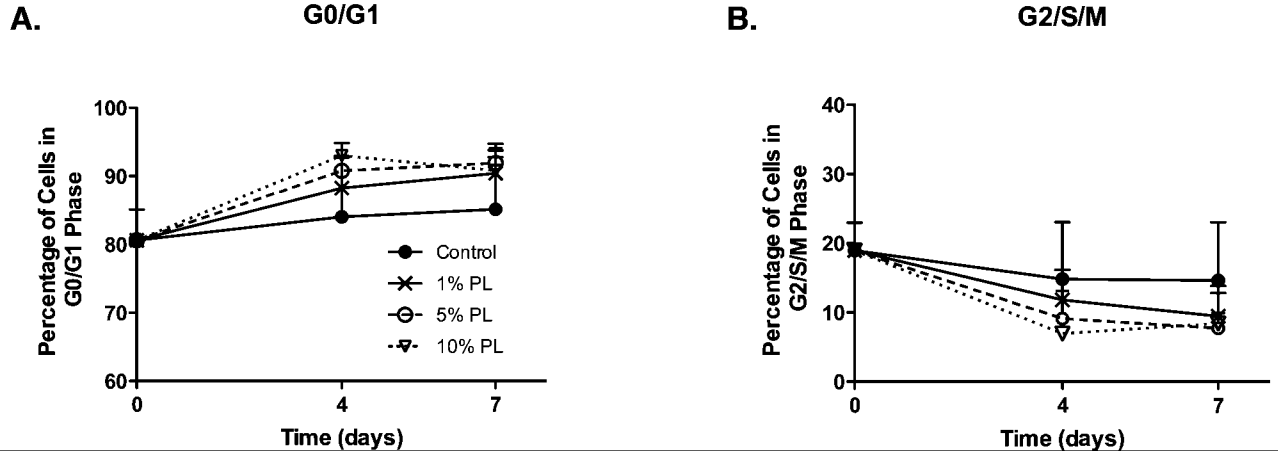
A.
G0/G1
Percentage of Cells in G0/G1 Phase
100
90
80
70
60
0
4
7
Time (days)
Control
1% PL
5% PL
10% PL
B.
G2/S/M
Percentage of Cells in G2/S/M Phase
40
30
20
10
0
0
4
7
Time (days)

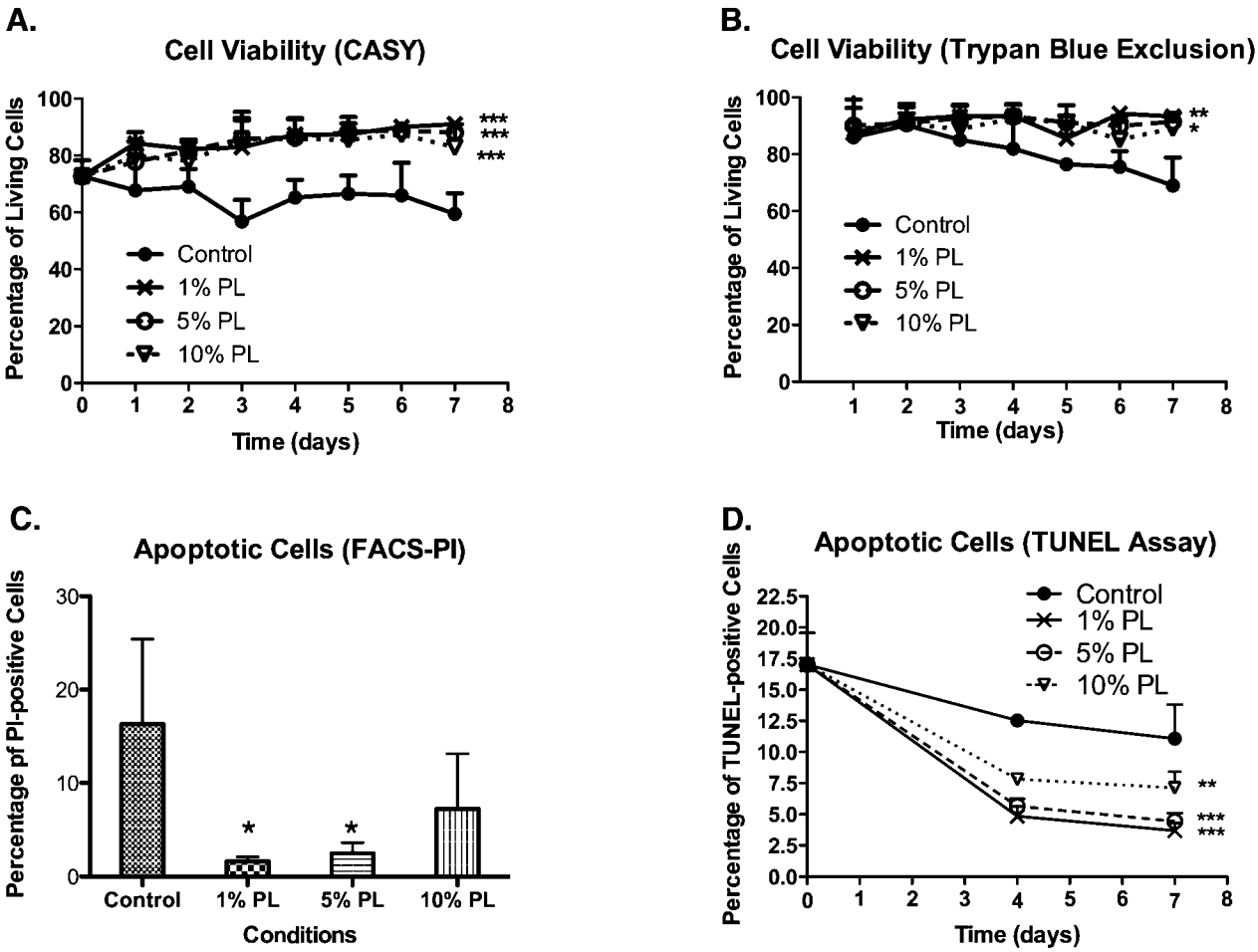
A.
Cell Viability (CASY)
Percentage of Living Cells
Time (days)
Control
1% PL
5% PL
10% PL
***
***
***
B.
Cell Viability (Trypan Blue Exclusion)
Percentage of Living Cells
Time (days)
Control
1% PL
5% PL
10% PL
**
*
C.
Apoptotic Cells (FACS-PI)
Percentage pf PI-positive Cells
Control
1% PL
5% PL
10% PL
Conditions
*
*
D.
Apoptotic Cells (TUNEL Assay)
Percentage of TUNEL-positive Cells
Time (days)
Control
1% PL
5% PL
10% PL
**
***
***

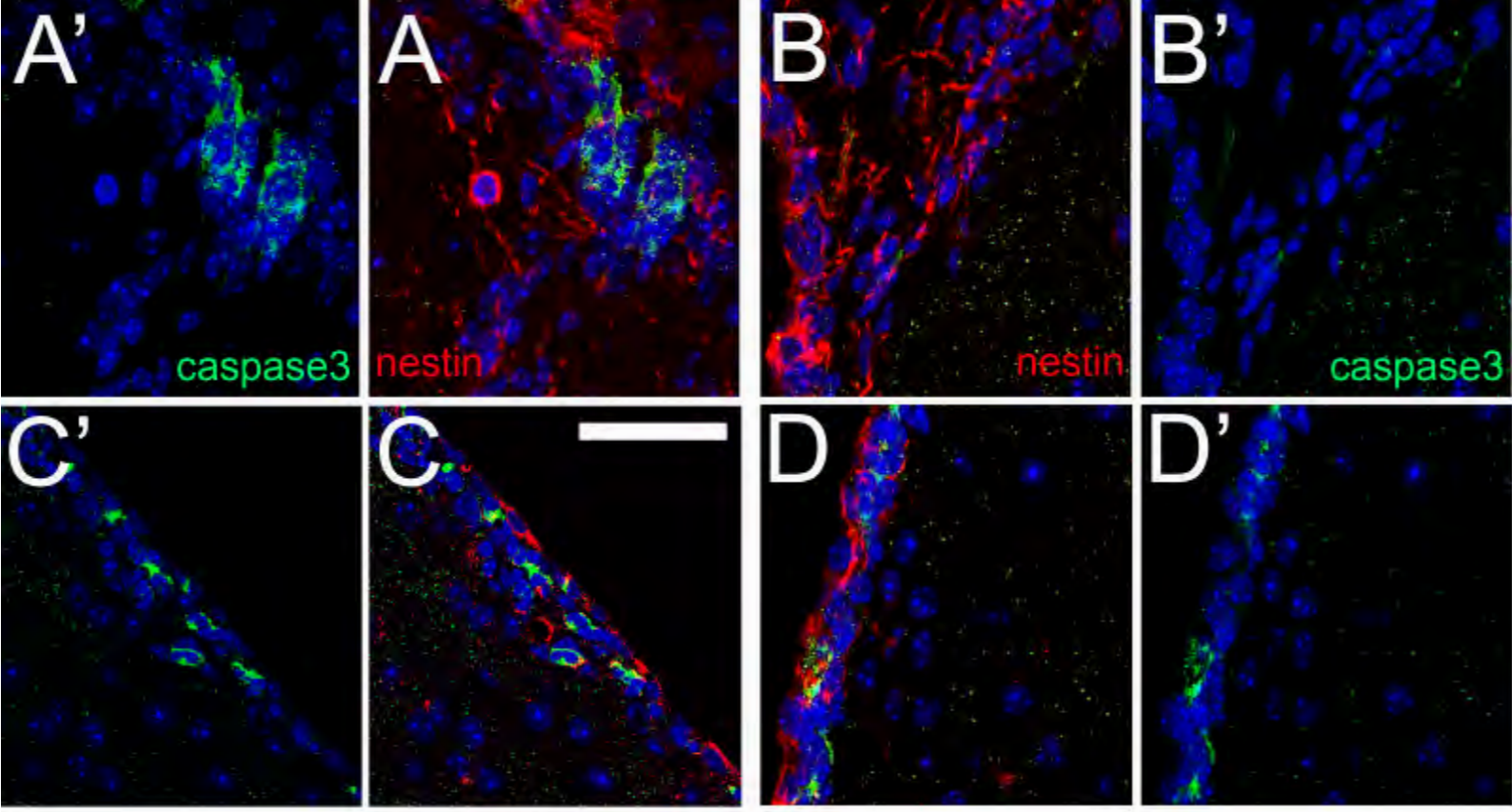
A'
caspase3
A
nestin
B
nestin
B'
caspase3
C'
C
D
D'

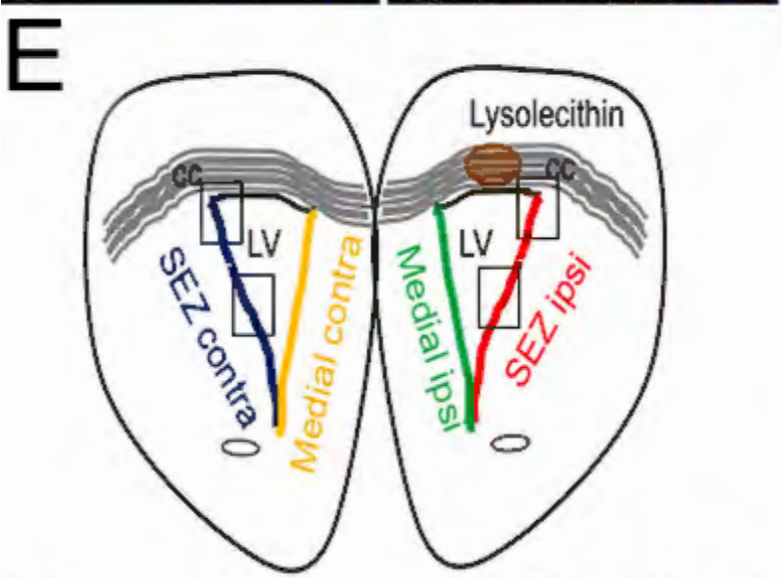
E
Lysolecithin
cc
cc
LV
LV
SEZ contra
Medial contra
Medial ipsi
SEZ ipsi

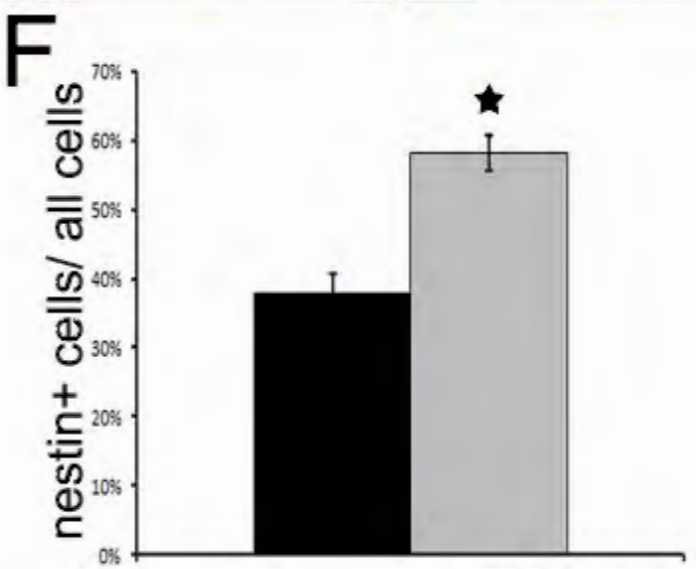
F
nestin+ cells/ all cells
70%
60%
50%
40%
30%
20%
10%
0%

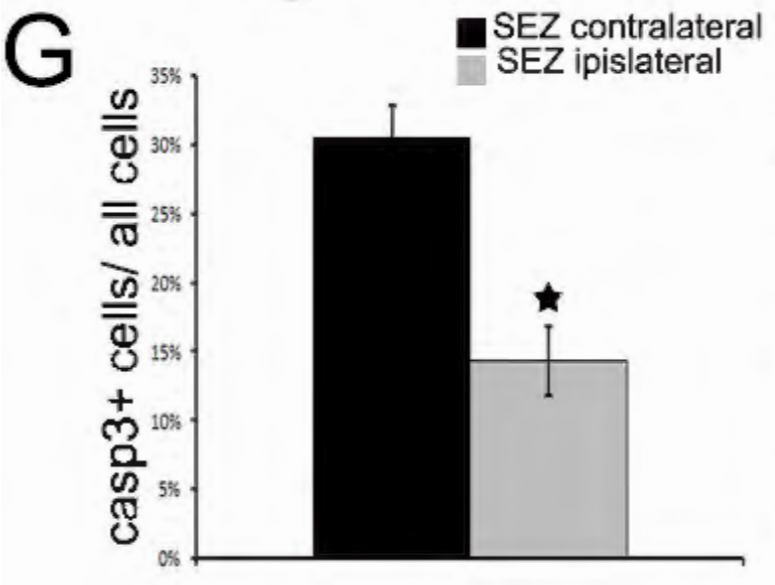
G
SEZ contralateral
SEZ ipislateral
casp3+ cells/ all cells
35%
30%
25%
20%
15%
10%
5%
0%

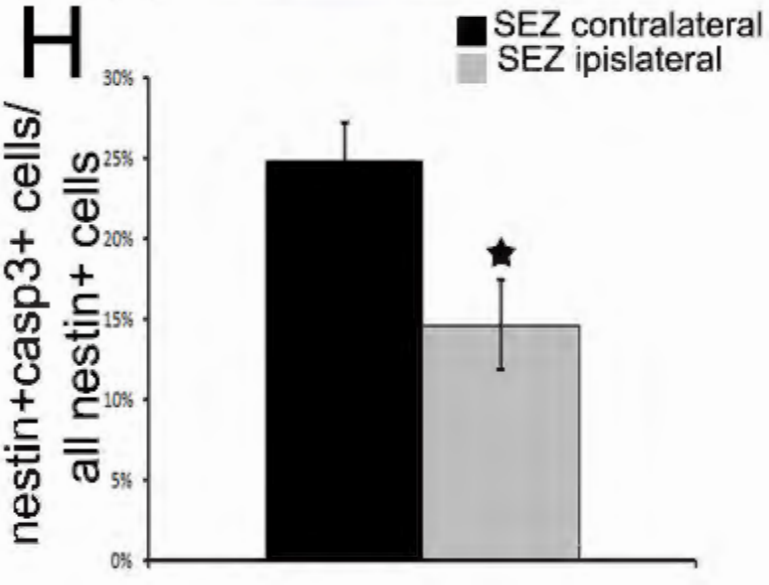
H
SEZ contralateral
SEZ ipislateral
nestin+casp3+ cells/ all nestin+ cells
30%
25%
20%
15%
10%
5%
0%